

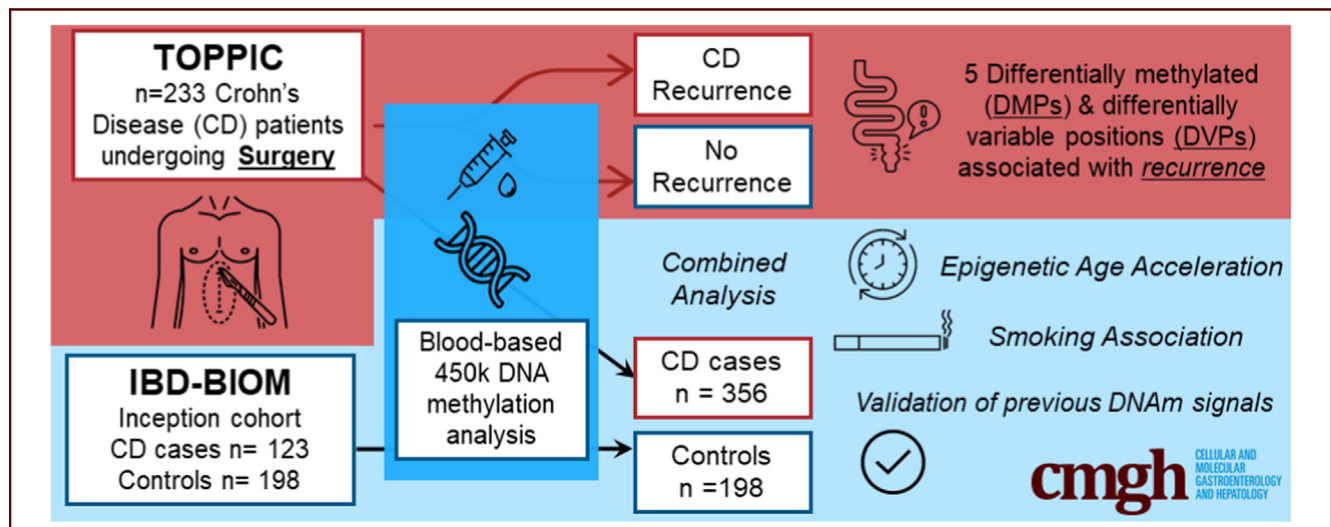
## ORIGINAL RESEARCH

## Genome-Wide Methylation Profiling in 229 Patients With Crohn's Disease Requiring Intestinal Resection: Epigenetic Analysis of the Trial of Prevention of Post-operative Crohn's Disease (TOPPIC)



Nicholas T. Ventham, Nicholas A. Kennedy, Rahul Kalla, Alex T. Adams, Alexandra Noble, Holly Ennis, TOPPIC Study Group, IBD-BIOM Consortium, Craig Mowat, Malcolm G. Dunlop, and Jack Satsangi

Centre for Genomic and Experimental Medicine, The University of Edinburgh, Edinburgh, Midlothian, United Kingdom



## SUMMARY

Detailed study of the circulating DNA methylome in adults with new and established Crohn's disease undergoing surgery within a large randomized controlled trial. Methylation alterations are observed in patients with post-operative disease recurrence.

**BACKGROUND & AIMS:** DNA methylation alterations may provide important insights into gene-environment interaction in cancer, aging, and complex diseases, such as inflammatory bowel disease (IBD). We aim first to determine whether the circulating DNA methylome in patients requiring surgery may predict Crohn's disease (CD) recurrence following intestinal resection; and second to compare the circulating methylome seen in patients with established CD with that we had reported in a series of inception cohorts.

**METHODS:** TOPPIC was a placebo-controlled, randomized controlled trial of 6-mercaptopurine at 29 UK centers in patients with CD undergoing ileocolic resection between 2008 and 2012. Genomic DNA was extracted from whole blood

samples from 229 of the 240 patients taken before intestinal surgery and analyzed using 450K Human Methylation and Infinium Omni Express Exome arrays (Illumina, San Diego, CA). Coprimary objectives were to determine whether methylation alterations may predict clinical disease recurrence; and to assess whether the epigenetic alterations previously reported in newly diagnosed IBD were present in the patients with CD recruited into the TOPPIC study. Differential methylation and variance analysis was performed comparing patients with and without clinical evidence of recurrence. Secondary analyses included investigation of methylation associations with smoking, genotype (MeQTLs), and chronologic age. Validation of our previously published case-control observation of the methylome was performed using historical control data (CD,  $n = 123$ ; Control,  $n = 198$ ).

**RESULTS:** CD recurrence in patients following surgery is associated with 5 differentially methylated positions (Holm  $P < .05$ ), including probes mapping to *WHSC1* ( $P = 4.1 \times 10^{-9}$ , Holm  $P = .002$ ) and *EFNA3* ( $P = 4.9 \times 10^{-8}$ , Holm  $P = .02$ ). Five differentially variable positions are demonstrated in the group of patients with evidence of disease recurrence including a probe mapping to *MAD1L1* ( $P = 6.4 \times 10^{-5}$ ). DNA methylation clock analyses demonstrated significant age acceleration in CD

compared with control subjects (GrimAge + 2 years; 95% confidence interval, 1.2–2.7 years), with some evidence for accelerated aging in patients with CD with disease recurrence following surgery (GrimAge +1.04 years; 95% confidence interval, -0.04 to 2.22). Significant methylation differences between CD cases and control subjects were seen by comparing this cohort in conjunction with previously published control data, including validation of our previously described differentially methylated positions (*RPS6KA2*  $P = 1.2 \times 10^{-19}$ , *SBNO2* =  $1.2 \times 10^{-11}$ ) and regions (*TXK* [false discovery rate,  $P = 3.6 \times 10^{-14}$ ], *WRAP73* [false discovery rate,  $P = 1.9 \times 10^{-9}$ ], *VMP1* [false discovery rate,  $P = 1.7 \times 10^{-7}$ ], and *ITGB2* [false discovery rate,  $P = 1.4 \times 10^{-7}$ ]).

**CONCLUSIONS:** We demonstrate differential methylation and differentially variable methylation in patients developing clinical recurrence within 3 years of surgery. Moreover, we report replication of the CD-associated methylome, previously characterized only in adult and pediatric inception cohorts, in patients with medically refractory disease needing surgery. (*Cell Mol Gastroenterol Hepatol* 2023;16:431–450; <https://doi.org/10.1016/j.jcmgh.2023.06.001>)

**Keywords:** Crohn's disease; Surgery; DNA methylation; Epigenetics; Inflammatory bowel disease; Aging.

**D**NA methylation is an important epigenetic mechanism that associates with alteration in gene expression with no underlying change in the genetic code. DNA methylation changes have been implicated in cancer; aging<sup>1–4</sup>; and many complex diseases, including inflammatory bowel disease (IBD).<sup>5,6</sup>

In our original studies, we described the circulating “methylome” in patients with IBD and control subjects,<sup>7,8</sup> including in a large inception cohort of newly diagnosed patients.<sup>9</sup> These methylation differences across the genome in peripheral blood leucocyte DNA correlate with known clinical parameters of inflammation, but importantly relate to underlying genotype. A key potential importance of DNA methylation changes relates to an association with alteration of gene expression. We were able to demonstrate the appropriate inverse relationship between methylation and gene expression, in a cell-specific manner in separated circulating leukocytes.<sup>9</sup> Most recently, we have provided strong replication of these methylation signals in a large inception cohort of patients with IBD recruited across Northern Europe, and replication of some signals in Southern Europe.<sup>10</sup>

Although genome-wide methylation differences have been demonstrated between IBD cases and control subjects, identifying methylomic differences between IBD subphenotypes is more nuanced. Multiomic data have also been used to prognosticate in IBD, attempting to delineate patients at risk of severe disease phenotype requiring surgery or more intensive drug regimens.<sup>11–15</sup> Using an unsupervised clustering method in our index study of an inception cohort of patients with Crohn's disease (CD) and ulcerative colitis, we identified groups of patients potentially at higher risk of surgery or treatment escalation.<sup>9</sup> In a large treatment-naïve inception cohort in Europe, we identified 3

methylation probes (*TAP1*, *TESPA1*, *RPTOR*) that associated with the need for treatment escalation to biologic agents or surgery.<sup>10</sup>

Patients with CD have a high lifetime risk of surgery for refractory or complicated disease. Approximately half of patients undergo surgery within 10 years of diagnosis;<sup>16</sup> however, with the introduction of newer biologic treatment, surgery rates seem to be falling.<sup>17</sup> The TOPPIC trial sought to determine the efficacy of 6-mercaptopurine (6-MP) in prevention of the recurrence of disease following ileocolic resection.<sup>18</sup> Two-hundred and forty patients were randomized across 29 UK centers to receive 6-MP or placebo following ileocolic resection for CD. The primary end point was a composite clinical end point that included an increase in Crohn's disease activity index score, requirement for treatment escalation, or further surgery. The trial showed a modest benefit with 6-MP treatment versus placebo for the primary clinical end point (hazard ratio, 0.54; 95% confidence interval [CI], 0.27–1.06). There was a more pronounced benefit for 6-MP for smokers (hazard ratio, 0.13; 95% CI, 0.04–0.46).<sup>18</sup>


The coprimary aims of the present study were to determine whether circulating DNA methylation differences in patients before surgery differ between patients with and without evidence of clinical or endoscopic recurrence following surgical resection; and to extend our observations of methylation alterations made in inception cohorts of newly diagnosed patients by studying an independent cohort of patients with established CD requiring surgery (Figure 1).

## Results

### Participants, Demographics, Data Processing, and Quality Control

There were 233 TOPPIC samples available for analysis with no samples failing quality control. Patient demographic information is presented for TOPPIC participants in Table 1. Data processing procedures demonstrated visually improved characteristics on density plots (Figure 2A–D) and multidimensional scaling (MDS) plots (Figure 2E–G). After filtering, 429,944 probes were available for analysis. No samples failed sex check (Figure 2F). QQ plots, Lambda values, and clustering of cohorts on MDS plots improved following combat correction (for both array number and intra-array position; Figure 3). Four TOPPIC patients had

**Abbreviations used in this paper:** 6-MP, 6-mercaptopurine; AHRR, aryl hydrocarbon receptor repressor; CD, Crohn's disease; CI, confidence interval; DMP, differentially methylated position; DMR, differential methylated region; DVP, differentially variable position; FDR, false discovery rate; IBD, inflammatory bowel disease; MDS, multidimensional scaling; meQTL, methylated quantitative trait loci; SNP, single-nucleotide polymorphism.

 Most current article

© 2023 The Authors. Published by Elsevier Inc. on behalf of the AGA Institute. This is an open access article under the CC BY license (<http://creativecommons.org/licenses/by/4.0/>).

2352-345X

<https://doi.org/10.1016/j.jcmgh.2023.06.001>

missing outcome data and were excluded from disease recurrence analyses.

In addition to the 233 novel TOPPIC samples described previously, there were 123 CD samples (combined = 356 CD samples) and 198 control subjects from the IBD-BIOM cohort.<sup>9</sup> Raw methylation from both cohorts (TOPPIC and BIOM) was normalized together. QQ plots, Lambda values, and clustering of cohorts on MDS plots improved following combat correction (for array number and intra-array position) between TOPPIC and BIOM cohorts (Figure 4). There were more than 40 technical replicates included across experimental batches with good visual clustering on MDS plots (Figure 5). Demographic details from the IBD-BIOM cohort are summarized in Table 2.

### DNA Methylation and Risk of Disease Recurrence Following Surgery in Patients With CD

**Differentially Methylated Positions.** There were 229 patients within the TOPPIC cohort available for comparison of the primary clinical end point of disease recurrence (n = 42) versus no recurrence. There were 5 statistically significant differentially methylated positions (DMPs) for the primary clinical end point, when including covariates (age, sex, smoking status, placebo/treatment, and estimated cell counts) and adjusting for multiple testing (Figure 6A, Table 3). DMPs are cg09916234 (*NSD2/WHSC1*,  $P = 4.07 \times 10^{-9}$ , Holm adjusted  $P = .002$ ), cg24864518 ( $P = 7.87 \times 10^{-9}$ , Holm adjusted  $P = .003$ ), cg06058618 (*EFNA3*,  $P = 4.92 \times 10^{-9}$ , Holm adjusted  $P = .02$ ), cg23939096 ( $P = 1.01 \times 10^{-7}$ ,

Holm adjusted  $P = .04$ ), and cg25981920 ( $P = 1.11 \times 10^{-7}$ , Holm adjusted  $P = .048$ ). When smoking is not included as a covariate in the linear model, there were 6 significant DMPs, with cg21472517 (*SAMD1*) in addition to the 5 outlined previously. There were no significant DMPs when comparisons of the endoscopic outcomes were used (data not shown).

**Differential Variable Positions.** Differential methylation variability was assessed using the iEVORA method comparing patients with disease recurrence and those without (using the clinical end point). There were 18 differentially variable positions (DVPs) associated with disease recurrence. When covariates were additionally used (age, sex, smoking status, cell proportions), there were 5 significant DVPs associated with disease recurrence (Figure 6B, Table 4). The 5 DVPs are cg24696067 (*MAD1L1*,  $P = 6.43 \times 10^{-6}$ ), cg02208776 (*HSPE1*,  $P = .001$ ), cg18068256 (*KRT37*,  $P = .02$ ), cg00475456 ( $P = .03$ ), and cg20310608 (*LOC284798*,  $P = .03$ ). There were no intersecting DMPs and DVPs associated with disease recurrence.

The biologic and functional relevance of DMPs and DVPs associated with CD recurrence following surgery are outlined in Table 5.

**Methylated Quantitative Trait Loci.** There were 216 samples with paired methylation and genotype data available for methylated quantitative trait loci (meQTL) analysis. The 5 DMPs and 5 DVP methylation probes were investigated for genotype association (meQTLs) using age, sex, and smoking status as covariates. There were 35 cis meQTLs with a false discovery rate (FDR;  $P < .05$ ), consisting of 35 different single-nucleotide polymorphisms (SNPs) and 7 of

**Table 1.** Patient Demographics of Patients Included From the TOPPIC Trial, With and Without Clinical Recurrence<sup>a</sup>

	Clinical recurrence (n = 40)	No recurrence (n = 189)	P value
Female, n (%)	26 (65.0)	115 (60.8)	.9
Age, y, median (IQR)	32.2 (27.8–41.0)	40.0 (29.0–49.8)	.02
Baseline CDAI (IQR)	124.5 (73.7–223.0)	112.0 (64.5–164.0)	.2
Disease location, n (%)			0.7
L1 ileal	14 (35.0)	74 (39.2)	
L3 ileocolonic	26 (65.0)	115 (60.8)	
Disease behavior, n (%)			0.8
Inflammatory B1	17 (42.5)	73 (38.9)	
Stricturing B2	17 (42.5)	89 (47.3)	
Penetrating B3	6 (15.0)	26 (13.8)	
Previous infliximab, n (%)	7 (17.5)	29 (15.7) (3missing)	1
Previous azathioprine, n (%)	22 (55)	102 (54.3)	1
Previous surgery, n (%)	9 (22.5)	62 (32.8)	.3
Current smoker, n (%)	14 (35)	40 (21.2)	.1
Biochemistry median (IQR)			
CRP, mg/L	3.7 (3–6)	4 (3–7)	.7
ESR	13 (6–22) (3 missing)	12 (5–19) (50 missing)	.4
Albumin	42 (41–46)	43 (40–45)	.8
White cell count	7.1 (5.5–8.5)	6.6 (5.5–8.1)	.4

NOTE. Results are presented as median, interquartile range. Nonparametric statistics are used to compare groups, chi-square for categorical data and Wilcoxon rank sum test for continuous data.

CDAI, Crohn's disease activity index; CRP, C-reactive protein; ESR, erythrocyte sedimentation rate; IQR, interquartile range; <sup>a</sup>Defined as increase in CDAI of more than 150 and an increase of 100 points from baseline measurement and institution of immunosuppressive treatment or further surgery.

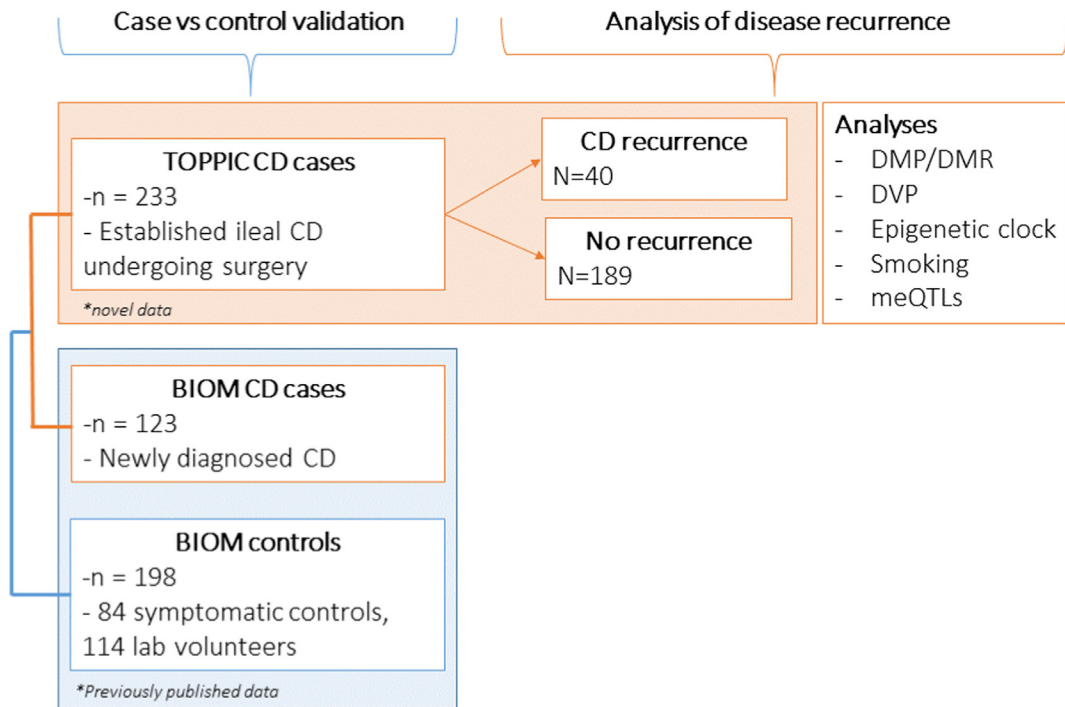


**Figure 1. Flowchart of cohorts and analyses.**

the 10 CpGs (Figure 9, Table 6). Three methylation probes had meQTLs associated with the primary end point of CD recurrence (with age, sex, and smoking status as covariates); cg00475456 (\*, DVP, rs7922288, FDR  $P = 4.89 \times 10^{-20}$ ), cg18068256 (DVP [KRT37] rs765335, FDR  $P = 2.80 \times 10^{-8}$ ), and cg24864518 (DMP, \*, exm669428, FDR  $P = 1.23 \times 10^{-5}$ ) (Table 7, Figure 10). Two DMPs (c09916234 [WHSC1/NSD2] and cg2484518) did not show any genetic association.

### Validation of DNA Methylation Changes in IBD Cases and Control Subjects

**TOPPIC CD Versus BIOM Control Subjects.** There were 19,179 DMPs (Holm adjusted  $P < .05$ ) associated with CD (TOPPIC,  $n = 233$ ) compared with BIOM control subjects ( $n = 198$ , in Table 8). Significant DMPs include our previously identified CD-associated DMPs including *RPS6KA2* (Holm adjusted  $P = 1.2 \times 10^{-19}$ ) and *SBNO2* (Holm adjusted  $P = 1.2 \times 10^{-11}$ ). Of the 412 CD-specific DMPs identified originally in Ventham et al,<sup>9</sup> 80 overlapped with the TOPPIC alone dataset (19.4%, with good correlation of log fold change values; Pearson correlation = 0.97). Using DMRCate, there were 4099 CD-associated differential methylated region (DMRs) with an FDR  $P < .00001$ . This included our previously described DMRs (*TXK* [FDR  $P = 3.6 \times 10^{14}$ ], *WRAP73* [FDR  $P = 1.9 \times 10^9$ ], *ITGB2* [FDR  $P = 1.4 \times 10^7$ ], and *VMP1* [FDR  $P = 1.7 \times 10^7$ ]).

**Combined Analysis of TOPPIC CD and BIOM CD Versus Control Subjects.** There were 4505 DMPs (Holm adjusted  $P < .05$ ) associated with CD ( $n = 356$ ) compared with control subjects ( $n = 198$ , top 20 DMPs presented in Table 9). The top DMP is *RPS6KA2* (Holm adjusted  $P = 1.4 \times 10^{-29}$ ), the principal finding from our previous work, and the

top 20 includes 2 probes within *SBNO2* (Holm adjusted  $P = 1.9 \times 10^{-18}$ ). There was 86.8% overlap (3909) of DMPs those identified using TOPPIC samples alone and the combined analysis with strong correlation of log fold change (Pearson correlation = 0.99). Using DMRCate, there were 812 CD-associated DMRs with an FDR  $P < .00001$ . This included our previously described DMRs (*TXK* [FDR  $P = 4.4 \times 10^{-12}$ ], *VMP1* [FDR  $P = 6.3 \times 10^{11}$ ], *WRAP73* [FDR  $P = 5.3 \times 10^8$ ], *ITGB2* [FDR  $P = 5.2 \times 10^7$ ]).

**Differentially Variable Positions (CD vs BIOM Control Subjects).** Differential variability was performed comparing CD cases (BIOM CD and TOPPIC) versus control subjects (BIOM control subjects) using the iEVORA method.<sup>28</sup> There were 18,993 DVPs hypervariable in CD compared with BIOM control subjects. Previously described IBD-associated DMPs were included as DVPs (*SBNO2*, var log 2 = 0.8,  $1.2 \times 10^{-32}$ ; *RPS6KA2*, var log 2 = 0.8,  $P = 5.5 \times 10^{-11}$  [uncorrected  $t$ -test]).

### Smoking and Epigenetic Age

**Smoking.** We performed a methylation analysis of smokers versus exsmokers and nonsmokers using the combined cohort ( $n = 554$ , regardless of case or control status). There were 169 methylation probes that associated with smoking (Holm corrected  $< 0.05$ ). Aryl hydrocarbon receptor repressor (*AHRR*) methylation has been strongly associated with smoking status and we confirm hypomethylation in current smokers (cg05575921, beta difference -10.8, Holm adjusted  $P = 5.46 \times 10^{-45}$ ; Figure 7A) with 5 *AHRR* probes in the top 20 most significant probes (cg05575921, cg21161138, cg26703534, cg14817490, cg25648203; Table 10).

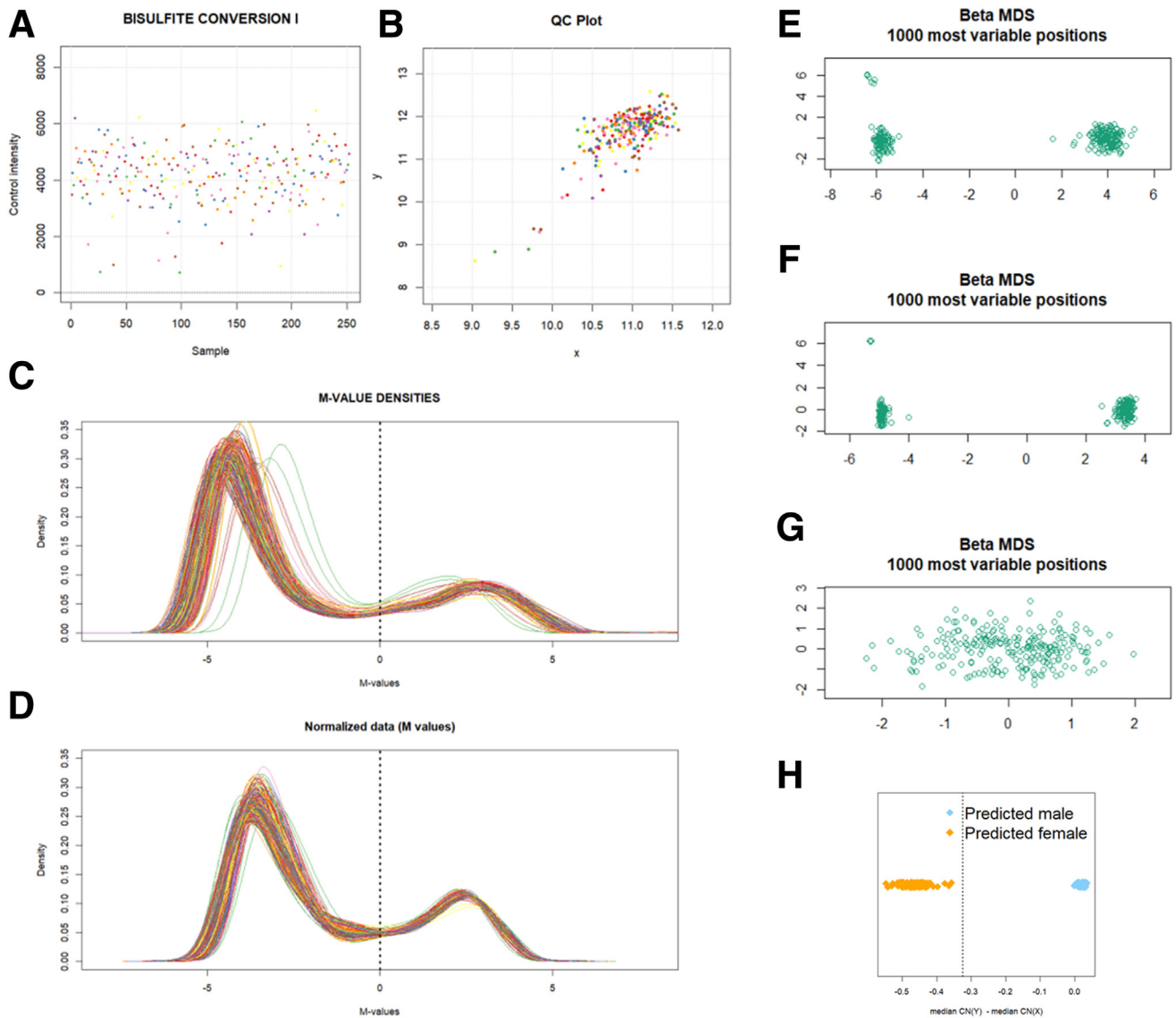


**Figure 2. ShinyMethyl output for quality control for TOPPIC methylation data.** (A) Average negative control probe intensities. (B) Median intensity of M channel against median intensity of the u channel. (C, D) M-value intensities before and after functional normalization. (E–G) MDS during processing steps. (E) Raw data. (F) Following quantile normalization. (G) Following filtering of SNPs and sex chromosomes. (H) ShinyMethyl sex-prediction plot. No samples were mismatched for sex.

Of the 169 significant probes, 137 (81%) have previously been described by Gao et al<sup>29</sup> in a meta-analysis of smoking-related probes. There was a modest but significant correlation in log fold difference in beta values here and published by Gao et al<sup>29</sup> (Pearson R = 0.4; Figure 7B).

To delineate CD-specific smoking associated methylation we then analyzed smoking-related methylation in CD cases (n = 356) and control subjects (n = 198) separately. There were 9 CpGs associated with smoking in patients with CD that did not overlap with the control or combined cohort or CpGs that had previously been described by Gao et al<sup>29</sup> (cg24497361, cg17777683, cg03088955, cg01218206, cg05895711, cg08006672, cg09273683, cg18688062, cg21963318; Figure 7C). When comparing these CD-specific smoking-associated CpGs, there were 4 overlapping probes compared with the CD case control DMPs described in the replication analyses

later (cg14753356, cg00295485, cg21963318, cg130338858; Figure 7D). The functional relevance of these smoking-related methylation probes is detailed in Table 11.

**Epigenetic Age.** Methylation age was calculated using the following methods: Horvath (DNAmAge),<sup>37</sup> Hannum,<sup>38</sup> phenoAge,<sup>39</sup> tissue specific (skin and blood clock),<sup>40</sup> and GRIMAge clocks.<sup>41</sup> All clocks demonstrated a strong and highly significant correlation with the biologic age, with the skin and blood clock demonstrating the strongest correlation (Pearson R = .96; 95% CI, 0.959–0.97;  $P < 1 \times 10^{16}$ ) (Figure 8A).

Epigenetic age acceleration is demonstrated in patients with CD compared with control subjects using all clocks (Figure 8B). When comparing age acceleration newly diagnosed patients with CD in the BIOM cohort with those with established disease requiring surgery in the TOPPIC cohort, there was some evidence of age acceleration in those

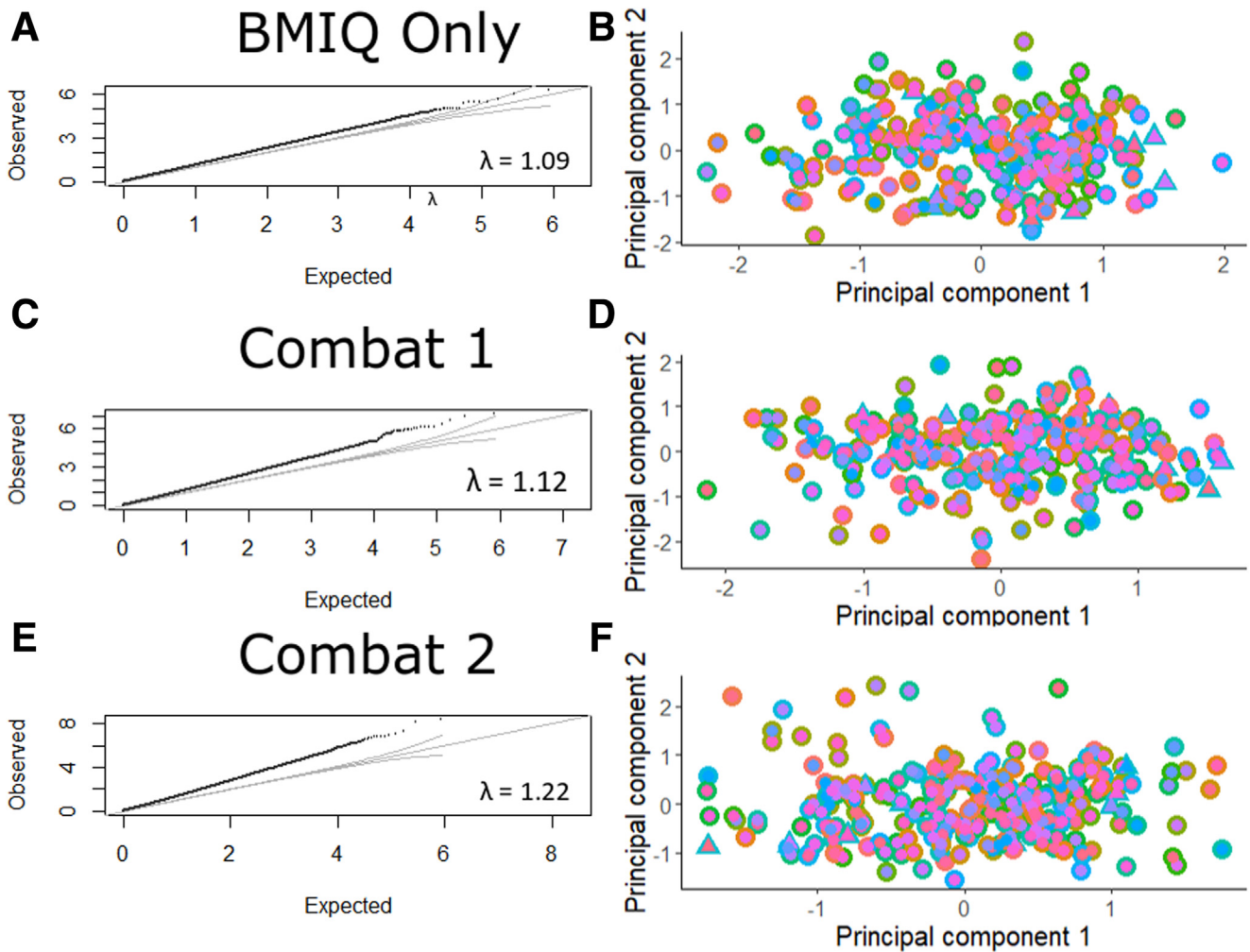


**Figure 3. Batch correction for TOPPIC-only methylation cohort.** (A, C, E) QQ plots and Lambda values for the (A) TOPPIC cohort following BMIQ and quantile normalization, (C) Combat correction for Chip (21 batches), and (E) Combat correction for position on array (12 batches). (B, D, F) Multidimensional scaling plots showing the first 2 principal components (B) TOPPIC cohort following BMIQ and quantile normalization, (D) Combat correction for Chip (21 batches), and (F) Combat correction for position on array (12 batches). *Inner color*, between array batch; *outer color*, intra-array batch; *triangles*, technical replicates.

requiring surgery using the DNAmAge clock, deceleration using the GrimAge clock, and no difference when using the other 3 clocks. The GrimAge clock also demonstrated some evidence of age acceleration in patients with disease recurrence following surgery compared with those without recurrence (+1.04 years; 95% CI, -0.04 to 2.22;  $P = .09$ ; Figure 8C). GrimAge acceleration strongly associated with smoking status (Figure 8D), but not inflammatory markers (C-reactive protein:  $r = 0.03$ ,  $P = .6$ ; albumin:  $r = 0.08$ ,  $P = .2$ ).

## Discussion

This study presents a detailed DNA methylation from a multicenter UK randomized controlled trial. We demonstrate differential methylation and differentially variable methylation in patients developing CD recurrence following surgery. Furthermore, the results strongly validate our previous studies,<sup>7-10</sup> describing methylation differences in IBD cases

versus control subjects, which had involved newly diagnosed patients, rather than those with established disease.

### Prediction of CD Recurrence Following Surgery

**DMPs.** The present study includes a unique and homogeneous cohort of patients with CD sampled before surgical resection and followed up within the rigorous confines of a randomized controlled trial with accurate clinical and endoscopic follow-up data. A smaller study with a similar cohort of patients postresection for ileal CD did not demonstrate systemic differences in DNA methylation in those experiencing a recurrence.<sup>42</sup> We demonstrate 5 significant DMPs following stringent correction for multiple testing. The significant DMPs include *EFNA3*, a tyrosine kinase receptor that plays a role in maintaining gut epithelial integrity and T-cell activation<sup>21</sup> and has been implicated in CD<sup>28</sup> and ulcerative colitis.<sup>23</sup> The ephrines have been postulated as potential therapeutic targets in CD.<sup>24</sup> *WHSC1/NSD2* is

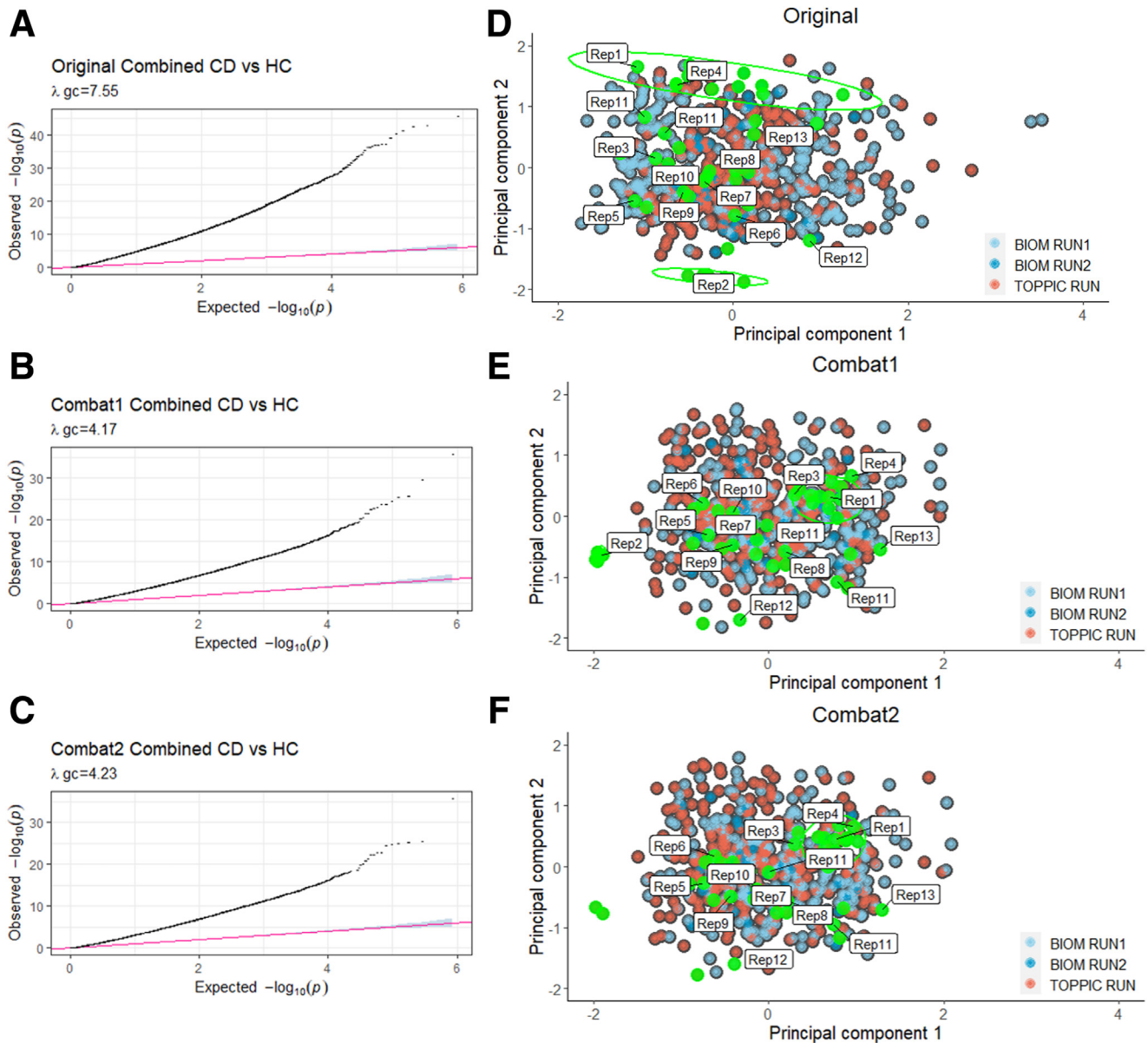


**Figure 4.** QQ plots and Lambda values for the originally combined TOPPIC and BIOM datasets following BMIQ and quantile normalization (A), followed by Combat correction for methylation chip (B) and location within each chip (C). MDS scaling plot of the first 2 principal components for the originally combined of TOPPIC and BIOM datasets following BMIQ and quantile normalization (D), followed by Combat correction for methylation chip (E), and location within each chip (F). Colors (blue, red) denote different experimental batches. Green labelled points denote technical replicates included across chips, plates, runs, and batches.

a nuclear binding domain associated with the condition Wolf-Hirschhorn syndrome. Notably the methylation probe exists close to a proinflammatory microRNA (mir-943).<sup>19</sup>

**DVPs.** Most epigenome-wide association studies have focused on case-control quantitative differences in DNA methylation at specific sites (DMPs). In the context of complex diseases such as IBD, the absolute differences in mean DNA methylation are often small (<5%), with unclear biologic consequence. There has been interest in measuring DNA methylation variability, or the pattern of variance at these sites. DVPs have been described as heterogeneous

outlier events and first described in cancer but increasingly described in complex diseases including T1 diabetes mellitus and rheumatoid arthritis twin studies.<sup>43,44</sup> We have identified 5 DVPs associated with disease recurrence following surgery. The most interesting DVP is *MAD1L1*, a mitotic arrest deficient 1 that represents a spindle assembly checkpoint between anaphase and metaphase. *MAD1L1* was a key finding in our previous work as a DMP that demonstrates IBD-specific appropriate inverse correlation between methylation and gene expression.<sup>10</sup> *MAD1L1* differential methylation has additionally been seen at the gut level,

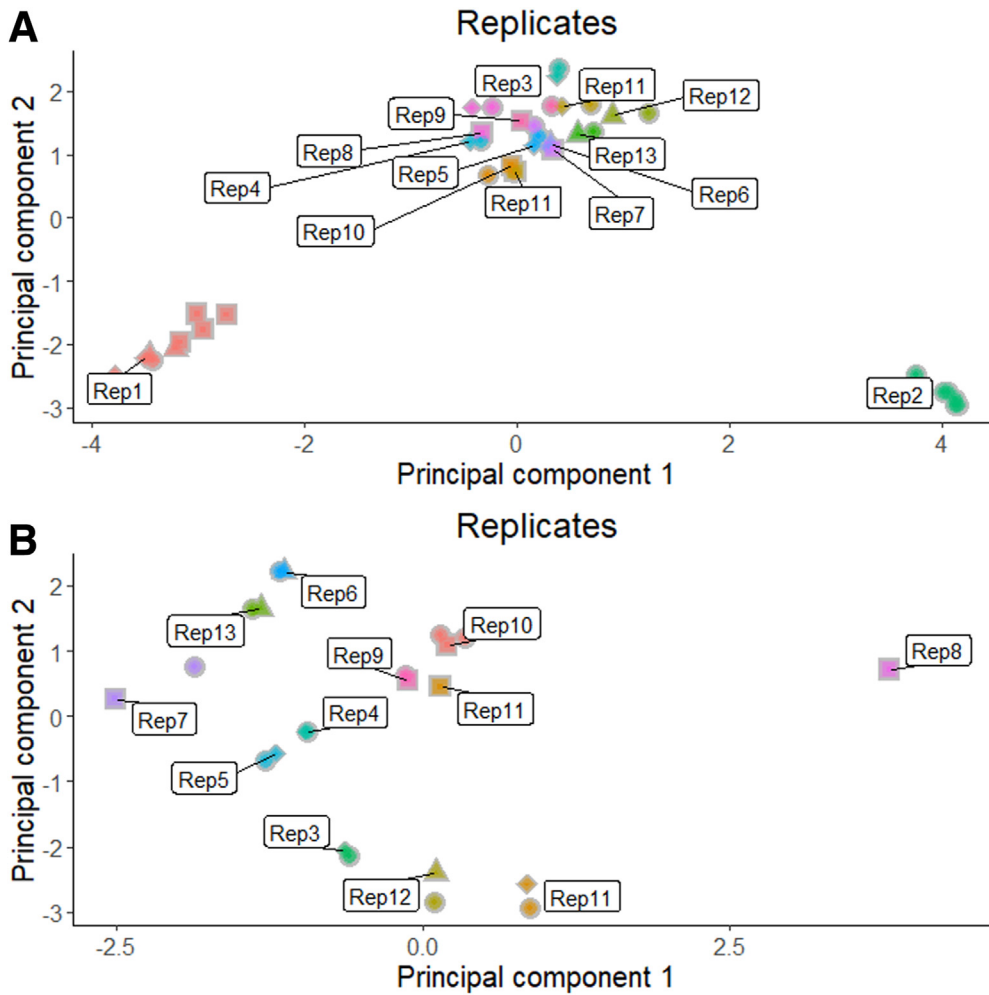


**Figure 5.** Principal component plot of the first 2 components (PC1, PC2) using 1000 most variable probes of the combined TOPPIC and BIOM cohorts. Colors correspond to technical replicates. Shapes refer to 450K scan date. (A) All replicates. (B) Replicates 1 and 2 removed.

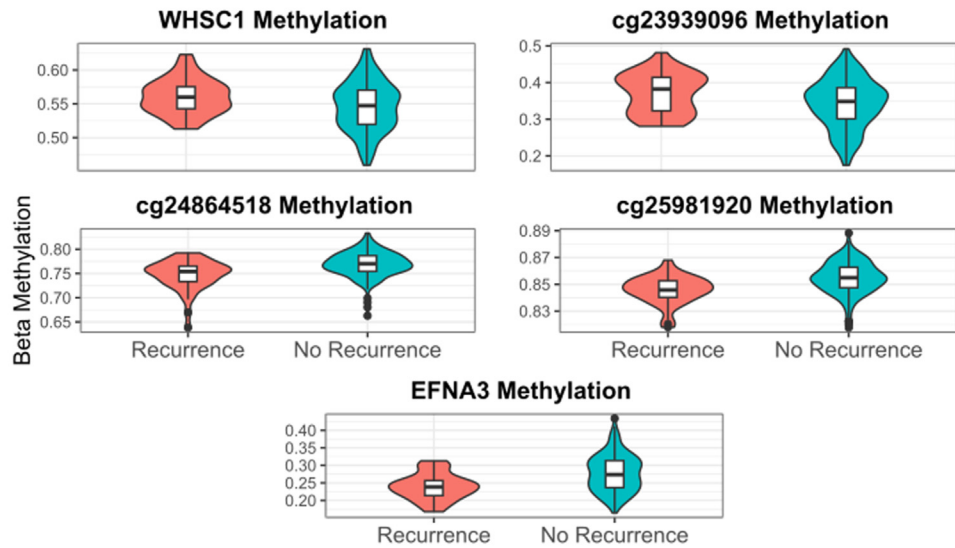
**Table 2.** Demographics of IBD-BIOM Validation Set

	CD (n = 123)	SC (n = 84)	P value SC vs CD	Healthy volunteers (n = 114)	P value HL vs CD
Age, median (IQR)	32.4 (24.9–50.7)	32.8 (26.4–45.5)	.9 <sup>a</sup>	32.3 26.4–40.6)	.4 <sup>a</sup>
Females, n (%)	58 (47.9)	39 (52.7)	.6 <sup>b</sup>	59 (50.4)	.8 <sup>b</sup>
Smoking status					
Current	53	17	Current vs ex/never	24	Current vs ex/never
Ex	29	17	.005	32	.0005
Never	39	40	Ever vs never	56	Ever vs never
Unknown	0	0	.004	5	.008
CRP	8 (2–23)	0 (0–3.5)	.006 <sup>a</sup>		
ESR	18 (5–39)	6 (4.5–7.5)	.002 <sup>a</sup>		
FC	495 (135–828)	19 (19–37)	.0001 <sup>a</sup>		

CD, Crohn’s disease; CRP, C-reactive protein; ESR, erythrocyte sedimentation rate; FC, fecal calprotectin; HL, healthy laboratory volunteers; IQR, interquartile range; SC, symptomatic control subjects; UC, ulcerative colitis. Adapted with permission from Ventham et al.  
<sup>a</sup>Wilcoxon rank sum test.  
<sup>b</sup>Chi-square test.



## A Differentially methylated positions (DMPs)



## B

## Differentially variable positions (DVPs)

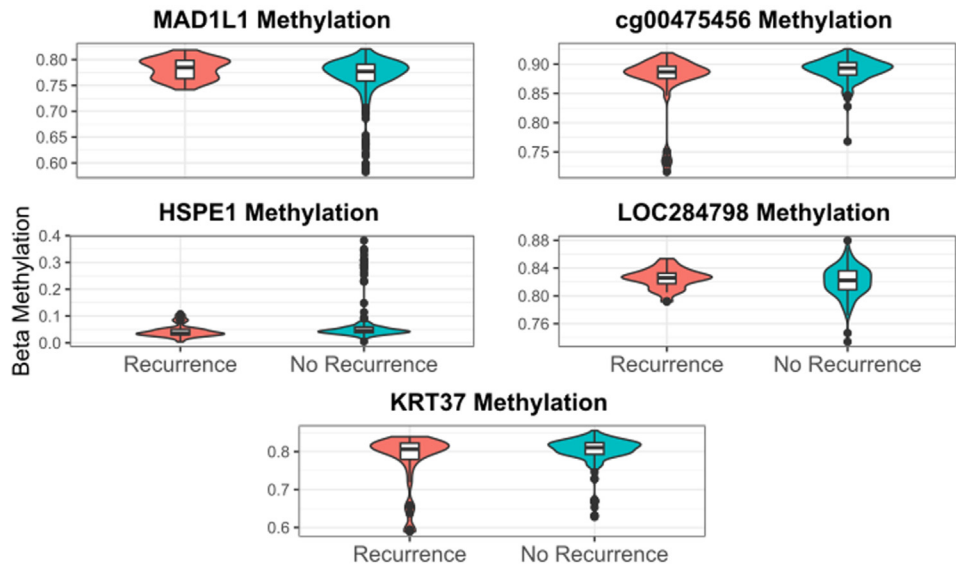


**Figure 6.** (A) Violin and box plots of DMPs associated with disease recurrence (clinical end point) following surgery for Crohn's disease. (B) Violin and box plots of DVPs associated with disease recurrence (clinical end point) following surgery for Crohn's disease (defined as increase in Crohn's disease activity index of more than 150 and an increase of 100 points from baseline measurement and institution of immunosuppressive treatment or further surgery).

within intraepithelial cells in ulcerative colitis.<sup>25</sup> The biologic significance of differential variability of methylation has not been well delineated. Unlike DMPs, DVPs lack clinical utility biomarkers because this technique relates to groups rather than individual patients.

**meQTLs.** Our group and others have previously demonstrated that genetic variation between IBD cases and control subjects relate to differential methylation,<sup>9,10,13</sup> raising the possibility that methylation may be a mediator of genetic susceptibility. Key DMRs including *VMP1* and *ITGB2* have been shown to be meQTLs.<sup>8,10</sup> In the present

study, there was a cis-genetic association in 8 of 10 methylation sites of interest (5 DMPs and 5 DVPs). Three meQTLs were associated with disease outcome (cg00475456, cg18068256, cg24864518; Figure 10); however, it is likely that differences are driven by small differences in allele frequency in patients with or without disease recurrence.

**Smoking.** There is a very strong relationship between smoking and CD susceptibility,<sup>45</sup> behavior,<sup>46</sup> and with postsurgical recurrence;<sup>47</sup> indeed in the TOPPIC trial, smoking habit was not only a determinant of recurrence;

**Table 3.** The 5 Holm Corrected Significant Differentially Methylated Positions Associated With Disease Recurrence Versus No Recurrence in Patients Undergoing Surgery for Crohn's Disease

	logFC	sym	Feature	P value	Holm adjusted P value
cg09916234	0.023	WHSC1	Body	4.07E-09	.002
cg24864518	-0.026	*	None	7.87E-09	.003
cg06058618	-0.046	EFNA3	Body	4.92E-08	.021
cg23939096	0.017	*	None	1.01E-07	.043
cg25981920	-0.010	*	None	1.11E-07	.048

Feature, location of methylation probe in relation to nearby gene on the 450K annotation manifest; logFC, log fold change; sym, gene symbol associated with methylation probe on the 450K annotation manifest.

but also was unexpectedly associated with the efficacy of thiopurine therapy.<sup>18</sup> The mechanism is uncertain, but given the significant effects of smoking on DNA methylation,<sup>29,30,32</sup> the relationship between smoking, CD, CD recurrence after surgery, and DNA methylation is of particular interest. Using the entire cohort (CD and control subjects), we were able to replicate the previously published smoking-related methylation probes<sup>29,30,32</sup> and correlate beta fold differences between smokers and non-smokers in ours and published series.<sup>38</sup> AHRH methylation has been strongly associated with smoking status and we confirm hypomethylation in current smokers (beta difference -10.8; Holm adjusted  $P = 5.46 \times 10^{-45}$ ) with 5 AHRH probes in the top 20 most significant probes. We then looked to identify smoking-associated probes that were present in patients with CD (and not control subjects). There were 3 CD-specific smoking-related probes that had not been associated with smoking in other published series. One probe mapped to *JOSD1* (cg03088955), a disubiquitination enzyme with a role in autophagy,<sup>33</sup> and another mapped to *PIP4KA2* (cg09273683), a gene with an SNP that was found to be an environmental interactor between smoking and colorectal cancer.<sup>35</sup>

**Epigenetic Clock.** DNA methylation data can be used to predict the biologic age of patients/samples and DNAm age acceleration is associated with mortality and a poorer prognosis in a range of conditions.<sup>48,49</sup> In the present dataset, we have used an online tool (Clock foundation) to calculate epigenetic age using a range of more recently

developed methylation clocks. We observe DNAm age acceleration in patients with CD compared with control subjects, replicating the same finding in our previous work.<sup>10</sup> Using the GrimAge clock we also demonstrate some evidence of epigenetic age acceleration in patients with CD recurrence following surgery, a finding not observed when using the other clocks. GrimAge may outperform the other clocks when predicting all-cause mortality and other age-related morbidity (healthspan).<sup>50</sup> The GrimAge clock was developed to include DNAm-based surrogate markers for smoking and other plasma proteins.<sup>41</sup> Epigenetic age acceleration occurs following major surgery, in particular following emergency hip fracture surgery, but returns to baseline 4–7 days following surgery.<sup>51,52</sup> Of more relevance, elective colorectal surgery was not associated with epigenetic age acceleration.<sup>51,52</sup> GrimAge acceleration associating with smoking and CD recurrence, but not traditional markers of inflammation, is particularly interesting given that smoking was found to be an important factor for disease recurrence in the original TOPPIC study.

#### Replication of CD Versus Control Subjects (Case vs Control)

A significant strength of this large DNA methylation dataset was the ability to validate our previous findings of differential methylation occurring in IBD cases and control subjects.<sup>9</sup> Critically, this demonstrates validation in a distinct cohort of patients recruited across multiple sites

**Table 4.** Top Table of Differentially Variable Positions in Patients With Disease Recurrence Postresection for CD Using Clinical End Point<sup>a</sup>

	Gene symbol	Chr	Feature	Mean beta no recurrence	Mean beta recurrence	Mean diff	P value.t
cg24696067	MAD1L1	7	Body	-0.003	0.015	0.018	6.43E-05
cg02208776	HSPE1	2	1stExon	0.004	-0.018	-0.022	0.001
cg18068256	KRT37	17	Body	0.005	-0.022	-0.026	0.024
cg00475456	*	1		0.003	-0.014	-0.017	0.027
cg20310608	LOC284798	20	TSS200	-0.001	0.003	0.004	0.031

NOTE. Calculated with the iEVOR method. A matrix of residual methylation values of a linear model including the following covariates was used (age, sex, smoking status, treatment/placebo, cell proportions).

<sup>a</sup>Defined as increase in Crohn's disease activity index of more than 150 and an increase of 100 points from baseline measurement and institution of immunosuppressive treatment or further surgery.

**Table 5.** Functional and Biologic Relevance of Significant Differential Methylated Positions and Differentially Variable Positions Associated Crohn's Disease Recurrence Following Surgery

Probe	Symbol	Function/relevance in inflammatory bowel disease
Differentially methylated probes		
cg09916234	NSD2/ WHSC1	Nuclear receptor binding SET domain protein 2. Wolf-Hirschhorn syndrome, a multisystem chromosomal disorder associated with a deletion on chromosome 4. Also the probe maps close to the transcription start site of microRNA-943 that has been shown to accelerate airway inflammation in asthma. <sup>19</sup>
cg24864518	*	This probe maps to an intergenic region close to the TSS of RASGEF1b, a guanine nucleotide exchange factor for Rap2, a member of the family of Rap G-protein signalling. <sup>20</sup>
cg06058618	EFNA3	Ephrine A3. Tyrosine kinase family of receptors. Ephrine-mediated repulsion of cells have a role in maintaining the integrity of the gut epithelial layer and may modulate T-cell activation. <sup>21</sup> Have previously been implicated in Crohn's disease <sup>22</sup> and ulcerative colitis, <sup>23</sup> and have been postulated as a potential therapeutic target in Crohn's disease. <sup>24</sup> Also extensively implicated in gastric and hepatocellular cancers. Target of miR-210-3p.
cg23939096	*	Maps to a noncoding area.
cg25981920	*	Maps to a noncoding area close to LY6L lymphocyte antigen6 family member.
Differentially variable probes		
cg24696067	MAD1L1	Mitotic arrest deficient like 1 acts as a spindle assembly checkpoint between metaphase and anaphase. <i>MAD1L1</i> was a key finding in our previous work that demonstrated IBD-specific correlation between DNA methylation and gene expression. <sup>10</sup> A different probe mapping to <i>MAD1L1</i> was differentially methylated in colonic intraepithelial cells in UC. <sup>25</sup> Because of its role in regulating the cell cycle, <i>MAD1L1</i> is also implicated in a variety of cancers.
cg02208776	HSPE1	Heat shock protein family E that acts a chaperonin. Implicated in colorectal cancer. <sup>26,27</sup>
cg18068256	KRT37	Keratin 37, a type I keratin that dimerises with type II keratins to form hair and nails.
cg00475456	*	Maps to an intergenic region close to PLXNA2 a plexin related in axon/nervous system development.
cg20310608	LOC284798	Uncharacterized LOC284798/ENSG00000230725.

IBD, inflammatory bowel disease; UC, ulcerative colitis.

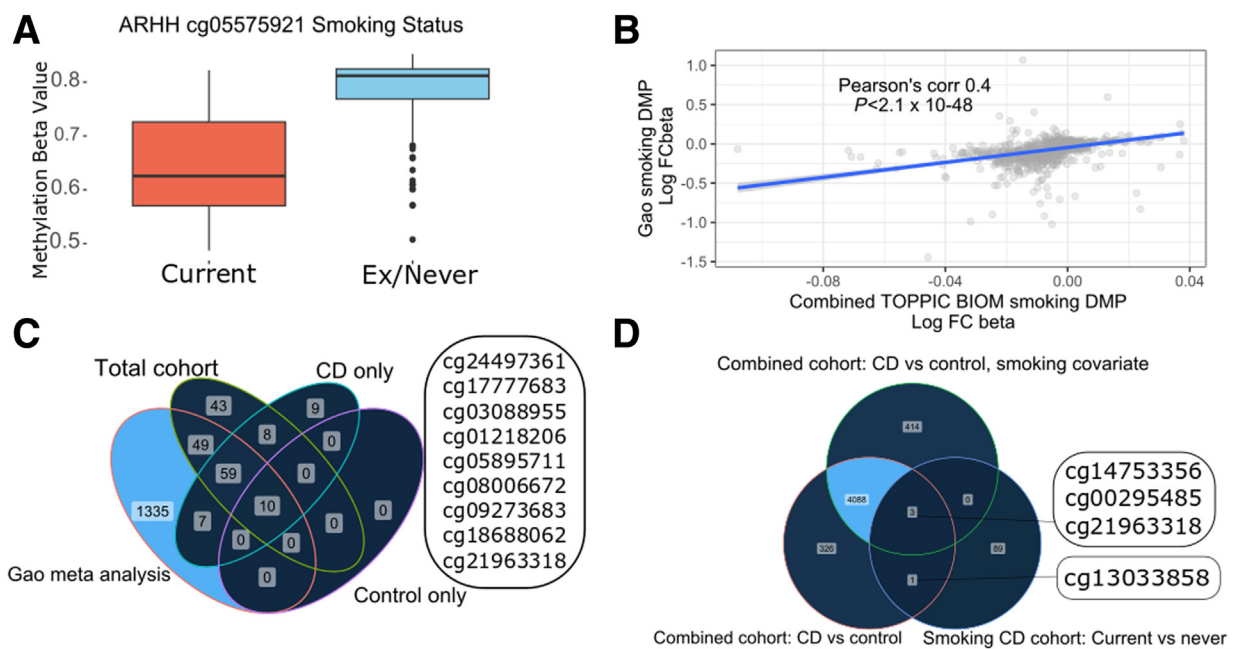


**Figure 7. (A)** Aryl hydrocarbon receptor repressor ARHH/cg05575921 methylation in smokers and nonsmokers and exsmokers in the entire cohort (combined CD and control subjects in both cohorts). **(B)** Correlation plot between smoking and exsmoker/nonsmoker log fold change beta value in Gao et al meta-analysis and in the present study (DMPs, Holm  $P < .05$ , entire cohort CD and control subjects combined). **(C)** Venn diagram of overlapping probes in Gao et al meta-analysis, smokers versus nonsmokers (DMPs, Holm  $P < .05$ ) in total cohort (CD and control subjects combined), Crohn's disease patients only, and control subjects only. The 9 smoking-associated CpGs seen only in the Crohn's cohort are listed in the box. **(D)** Venn diagram of Crohn's disease versus control DMPs in the entire cohort without using smoking as a covariate, entire cohort using smoking as a covariate, and in the smoking-associated DMPs in the Crohn's only cohort. There are 4 CpGs that overlap that are both associated with Crohn's (vs control, DMPs) and smoking (smoking vs exsmoker/never smoker, DMPs) that are listed in the boxes.

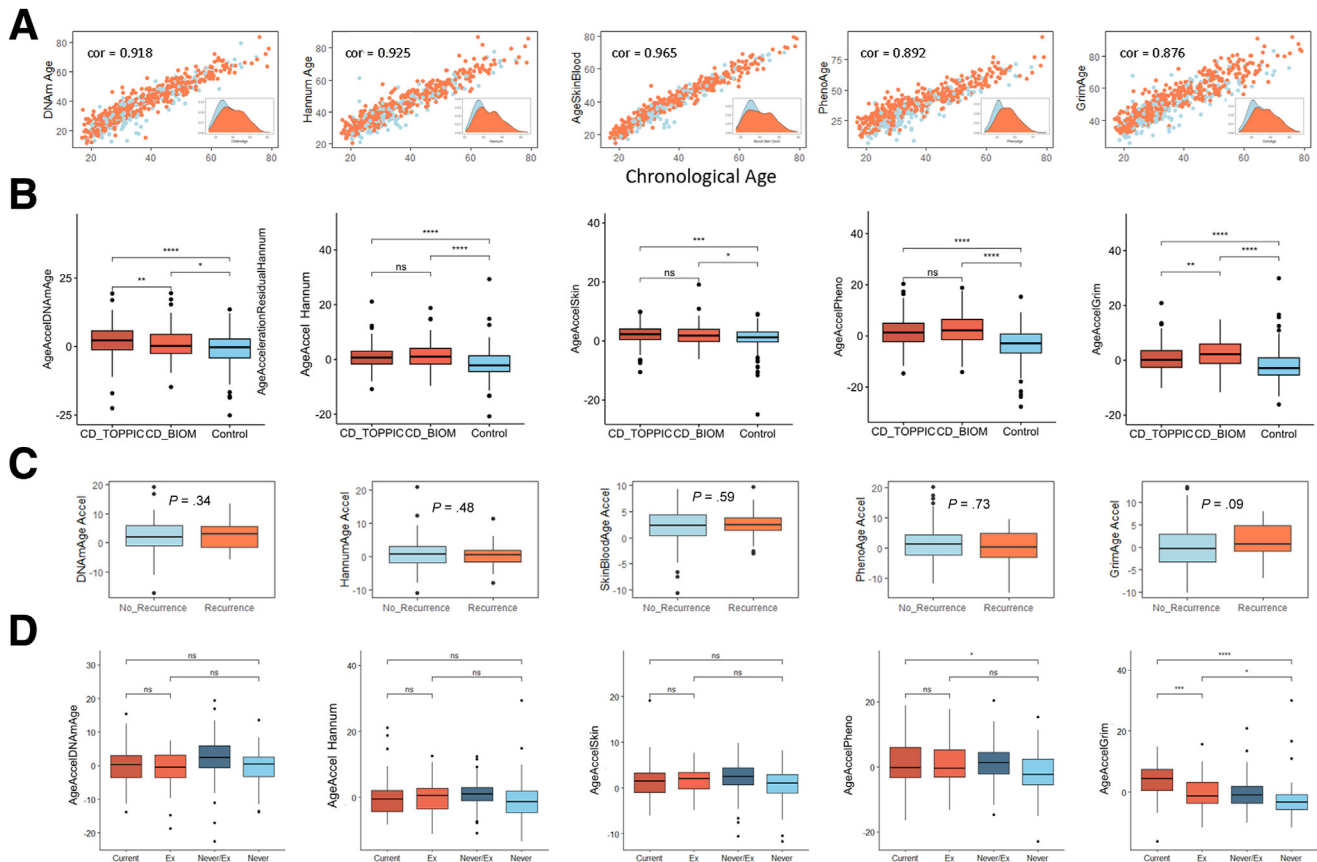


**Figure 8. Epigenetic age analysis using methods by (from right to left) Horvath (DNAmAge),<sup>40</sup> Hannum,<sup>41</sup> tissue specific (skin and blood clock),<sup>21</sup> phenoAge,<sup>42</sup> and GRIMAge clocks.<sup>22</sup> (A) Correlation plot of methylation age (y-axis) and biologic age (x-axis) using methods above, inset, density plot of methylation age). Cor, Pearson's R Correlation estimate. (B) Boxplots of age acceleration using methods above in patients with Crohn's disease requiring surgery (CD\_TOPPIC), newly diagnosed Crohn's disease patients (CD\_BIOM), and control subjects. (C) Boxplots of age acceleration in patients included in the TOPPIC trial who went on to develop recurrence or no recurrence following surgery. (C) Box plot for each methylation clock age acceleration and smoking status, current, exsmoker (recorded in the BIOM cohort), exsmoker/never smoker (grouped together as part of the TOPPIC cohort), and never smoked (recorded in the BIOM cohort). Ns =  $P > .05$ , \* $P < .05$ , \*\* $P < .01$ , \*\*\* $P < .001$ , \*\*\*\* $P < .0001$  (Wilcox test).**

across the United Kingdom. Whereas our previously published case-control analyses involved newly diagnosed patients,<sup>9</sup> the TOPPIC cohort consists of patients with established disease. Using TOPPIC data we replicated our previous key DMPs *TXK* (FDR  $P = 3.6 \times 10^{14}$ ), *WRAP73* (FDR  $P = 1.9 \times 10^9$ ), *VMP1* (FDR  $P = 1.7 \times 10^7$ ), and *ITGB2* (FDR  $P = 1.4 \times 10^7$ ). Data from the RISK cohort, a treatment-naïve pediatric inception cohort, demonstrated a tendency for most methylation signals to revert following treatment,<sup>13</sup> notably with the exception of IBD-associated *RPS6KA2* hypomethylation, a finding replicated in using this novel cohort (Holm adjusted  $P = 1.2 \times 10^{-19}$ ). Data from this present study suggest either that these methylation findings may either endure from diagnosis or, alternatively, be present; resolve in remission; and recur in patients with uncontrolled disease reflecting active inflammation at time of sampling. Although the present study cannot address these issues, longitudinal analysis suggest that for most the loci, resolution may occur with disease

control; in a small proportion, including notably *RPSKA2*, the changes may be constant regardless of inflammatory status.<sup>13</sup> This area is under further analysis.

### Differential Variable Positions

In this study, we describe CD-associated differentially variable methylation for the first time in IBD versus control subjects. The enrichment of DMPs and DMRs is an artefact of the analytical technique, with the iEVORA method ranking DVPs higher if a DMP at genome-wide significance level or as close to possible to a DMP.<sup>28</sup> Variable methylation has been hypothesized to account for differences in disease susceptibility among individuals and between ethnicities.<sup>53</sup> It has been noted in healthy individuals that there is higher variability in specific regions of genome, and in particular in immune-related pathways, and low variability in highly conserved regions associated with basic cellular functions.<sup>54</sup> The pathobiologic significance of the DVPs described here warrants further investigation.

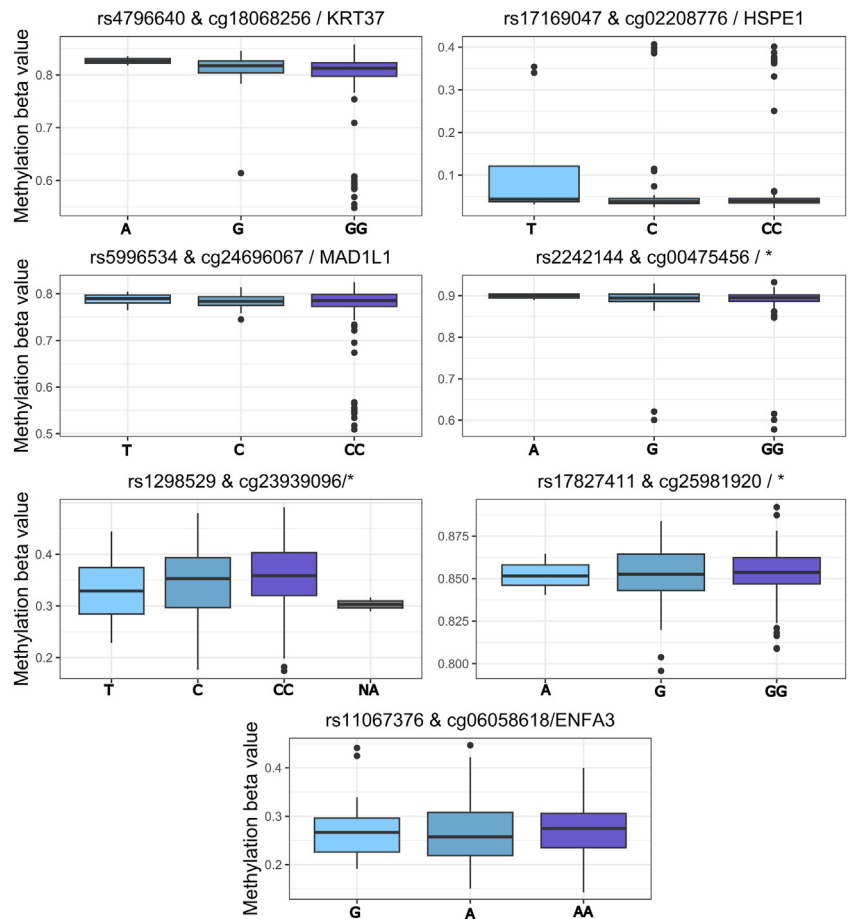


**Figure 9.** cis meQTLs of DVP/DMP probes. Top SNP shown. Age, sex, smoking status used as covariates. MAF of <10% filtered. Cis distance  $1 \times 10^6$ ,  $P$  value threshold  $<2 \times 10^{-6}$ .

**Strengths and Limitations**

This is a large dataset of phenotypically homogenous patients with IBD with established disease and provides complementary information to our previously published work in newly diagnosed patients. The combined datasets provide one of the largest series genome-wide DNA methylation data in CD to date and provides compelling replication of our previous key findings in a novel dataset

of patients with established disease. The TOPPIC trial was a well-conducted randomized controlled trial performed across multiple sites across the United Kingdom with well-phenotyped data and accurate follow-up data to 3 years. Raw data were normalized together and included more than 40 technical replicate samples performed across chip positions and across separate methylation runs for each separate cohort (TOPPIC,

**Table 6.** Top Cis meQTLs Associated With DMP (black) and DVP (grey) Methylation Probes, Most Significant SNP is Listed (age, sex, smoking status used as covariates)

SNP	Methylation probe/annotation symbol	Statistic	$P$ value	FDR corrected $P$ value	beta
rs4796640	cg18068256 / KRT37	8.2	1.77E-14	9.33E-08	0.07
rs17169047	cg02208776 / HSPE1	-6.2	2.34E-09	0.003	-0.06
rs5996534	cg24696067 / MAD1L1	5.5	1.32E-07	0.09	0.04
rs2242144	cg00475456 /*	5.4	1.48E-07	0.09	0.03
rs1298529	cg23939096/*	5.3	2.50E-07	0.09	0.04
rs17827411	cg25981920 /*	5.2	3.87E-07	0.12	0.01
rs11067376	cg06058618 / ENFA3	5.0	1.16E-06	0.24	0.03

NOTE. MAF of <10% filtered. Cis distance  $1 \times 10^6$ ,  $P$  value threshold  $<2 \times 10^{-6}$ . DMP, differentially methylated position; DVP, differentially variable position; FDR, false discovery rate; meQTL, methylated quantitative trait loci; SNP, single-nucleotide polymorphism.

**Table 7.** Top Cis meQTLs Associated With Clinical End Point (Disease Recurrence) DMP (black) and DVP (grey) Methylation Probes, Top SNP is Listed

SNP	Methylation probe	Statistic	<i>P</i> value	FDR corrected <i>P</i> value	Beta
rs7922288	cg00475456 /*	12.4	9.27E-27	4.89E-20	0.19
rs765335	cg18068256 / KRT37	7.6	1.30E-12	2.80E-08	0.23
exm669428	cg24864518 /*	6.2	2.64E-09	1.23E-05	0.10

NOTE. Age, sex, smoking status used as covariates. MAF of  $<10\%$  filtered. Cis distance  $1 \times 10^6$ , *P* value threshold  $<2 \times 10^{-6}$ . DMP, differentially methylated position; DVP, differentially variable position; FDR, false discovery rate; meQTL, methylated quantitative trait loci; SNP, single-nucleotide polymorphism.

BIOM), with appropriate clustering on MDS plots increasing the confidence of performing analyses across cohorts (Figure 5), limiting the impact of the control samples arising from 1 of the 2 datasets. Notwithstanding this, novel DMPs described in the TOPPIC CD versus BIOM control subjects require further replication. Despite rigorous correction and technical replicates, results from this analysis are likely to be overinflated, as noted by the number of positive DMPs in the TOPPIC CD versus control subjects being higher than in the combined analysis. The blood sample used for methylation analysis was taken before administration of the study treatment (6-MP) or placebo and will not affect the methylation data itself but may impact the studied outcome of disease recurrence (despite nonstatistically significant findings in original randomized controlled trial). RNA was not available to attempt to associate differential methylation variance and expression.

## Conclusions

We identify methylation changes present at the time of surgery that are associated with future CD recurrence within 3 years. Probes within the 5 site-specific (DMPs) and 5 DVPs associate with the underlying genotype and relate to genes with biologic relevance to CD. Given the relationship between smoking, methylation, and IBD, we have identified CD-specific smoking-related methylation sites. Replication of the CD-associated methylation alterations is achieved, having previously characterized only in adult and pediatric inception cohorts, in patients with well-established disease requiring surgery.

## Methods

### Datasets

TOPPIC was a placebo-controlled, randomized controlled trial of 6-MP at 29 UK centers in patients with CD

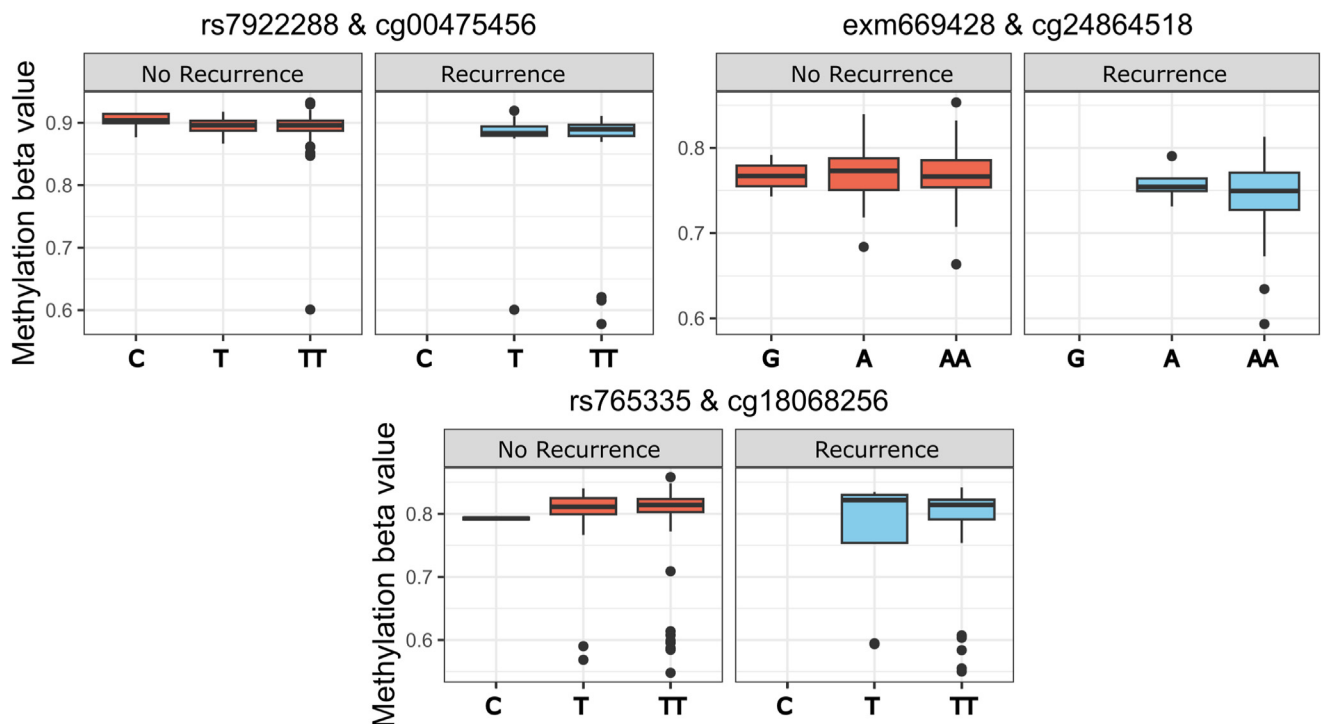


**Figure 10.** Cis meQTLs of DVP or DMP probes associated with Crohn's disease recurrence following surgery. Top SNP shown. Age, sex, smoking status used as covariates. MAF of  $<10\%$  filtered. Cis distance  $1 \times 10^6$ , *P* value threshold  $<2 \times 10^{-6}$ .

**Table 8.** Top 20 Differentially Methylated Positions Crohn's Disease TOPPIC (n = 233) Versus Control Subjects BIOM Dataset (n = 198)

	logFC	sym	Feature	P value	Adjusted P value
cg21155778	-0.10	FGD6	TSS200	8.65E-50	3.72E-44
cg17931986	0.07	COL11A2	3'UTR	2.23E-38	9.60E-33
cg19755108	0.03	UIMC1	TSS1500	1.96E-37	8.44E-32
cg19056176	-0.06	KIAA0513	5'UTR	1.21E-36	5.21E-31
cg14863978	-0.04	GBX1	TSS200	1.30E-36	5.58E-31
cg02159402	-0.09	GALNT11	TSS200	4.71E-36	2.03E-30
cg05410609	-0.07	CCDC85C	5'UTR	5.89E-35	2.53E-29
cg15281724	0.06	TXLNB	Body	1.94E-34	8.32E-29
cg19165344	0.03	AP1B1	TSS1500	2.82E-33	1.21E-27
cg04450857	-0.06	EMX2OS	Body	4.82E-33	2.07E-27
cg17541922	-0.04	PRSS23	5'UTR	7.18E-33	3.09E-27
cg18100079	0.04	*	None	1.49E-32	6.41E-27
cg02951344	-0.05	SYTL2	TSS200	3.66E-32	1.57E-26
cg14910854	0.03	LOC150776	Body	8.88E-32	3.82E-26
cg11338426	-0.05	CRHR1	1stExon	1.50E-31	6.45E-26
cg03047400	-0.06	*	None	3.04E-31	1.31E-25
cg18301538	0.04	GBF1	Body	3.47E-31	1.49E-25
cg21120539	-0.04	CTSZ	1stExon	3.79E-31	1.63E-25
cg06996129	-0.09	*	None	5.89E-31	2.53E-25
cg12216772	-0.07	ANUBL1	5'UTR	1.02E-30	4.39E-25

NOTE. Age, sex, smoking, estimate cell proportion included as covariates in linear model. Holm adjusted P value. logFC, log fold change.

**Table 9.** Combined-Analysis of Differentially Methylated Positions Crohn's Disease (TOPPIC and BIOM) Versus Control Subjects BIOM Dataset)

	logFC	sym	Feature	P value	Adjusted P value
cg17501210	-0.06	RPS6KA2	Body	3.15E-35	1.35E-29
cg21155778	-0.06	FGD6	TSS200	4.10E-26	1.76E-20
cg25422678	0.03	BRE	Body	3.06E-25	1.32E-19
cg24430034	0.03	*	None	4.15E-25	1.78E-19
cg18181703	-0.04	SOCS3	Body	1.86E-24	8.00E-19
cg18608055	-0.05	SBNO2	Body	4.39E-24	1.89E-18
cg03546163	-0.07	FKBP5	5'UTR	4.39E-22	1.89E-16
cg26955383	0.03	CALHM1	TSS200	4.90E-22	2.10E-16
cg26470501	-0.03	BCL3	Body	5.16E-22	2.22E-16
cg07573872	-0.05	SBNO2	Body	2.25E-21	9.66E-16
cg16411857	-0.04	NLRC5	TSS1500	2.61E-21	1.12E-15
cg12992827	-0.05	*	None	1.13E-20	4.84E-15
cg04975846	-0.05	TRAPPC2L	Body	5.67E-20	2.44E-14
cg07839457	-0.07	NLRC5	TSS1500	5.81E-20	2.50E-14
cg12269535	-0.04	SRF	Body	6.29E-20	2.71E-14
cg09090048	-0.04	VPS26B	TSS1500	7.91E-20	3.40E-14
cg11738543	-0.02	SOCS2	Body	2.54E-19	1.09E-13
cg02508743	0.03	LYN	Body	3.14E-19	1.35E-13
cg08791347	0.03	FRMD4A	Body	1.12E-18	4.83E-13
cg01839860	0.02	UBE2D2	5'UTR	1.99E-18	8.55E-13

NOTE. Age, sex, smoking, estimate cell proportion included as covariates in linear model. Holm adjustment for multiple testing. logFC, log fold change.

**Table 10.** Top 20 Smoking-Associated Methylation Probes

	logFC	P value	Adjusted P value	SYM	Feature
cg05575921	-0.108	1.27E-50	5.46E-45	AHRR	Body
cg01940273	-0.062	1.95E-41	8.38E-36	*	None
cg03636183	-0.072	1.38E-35	5.92E-30	F2RL3	Body
cg06126421	-0.071	1.24E-32	5.33E-27	*	None
cg05951221	-0.068	8.27E-31	3.56E-25	*	None
cg21161138	-0.040	6.87E-29	2.95E-23	AHRR	Body
cg26703534	-0.035	1.84E-28	7.89E-23	AHRR	Body
cg21566642	-0.056	2.24E-23	9.61E-18	*	None
cg03329539	-0.031	4.73E-22	2.03E-16	*	None
cg14817490	-0.043	2.91E-20	1.25E-14	AHRR	Body
cg25648203	-0.029	6.33E-20	2.72E-14	AHRR	Body
cg04885881	-0.040	7.50E-20	3.23E-14	*	None
cg09935388	-0.063	9.17E-19	3.94E-13	GFI1	Body
cg19572487	-0.033	3.40E-18	1.46E-12	RARA	5'UTR
cg07826859	-0.026	4.95E-17	2.13E-11	MYO1G	TSS1500
cg14753356	-0.035	5.37E-17	2.31E-11	*	None
cg25189904	-0.054	9.99E-17	4.30E-11	GNG12	TSS1500
cg07339236	-0.028	2.45E-16	1.05E-10	ATP9A	Body
cg00310412	-0.027	2.85E-16	1.22E-10	SEMA7A	Body
cg23079012	-0.024	7.46E-16	3.21E-10	*	None

NOTE. Linear model smokers versus exsmokers and nonsmokers including age, sex, and cell admixture as covariates. Data include all patients and control subjects in combined cohort (CD and control subjects). Adjusted P value is Holm correction for multiple testing. logFC, log fold change.

undergoing ileocolic resection between 2008 and 2012.<sup>18</sup> Genomic DNA was extracted from whole blood samples from 229 of the 240 patients taken before intestinal surgery. The IBD-BIOM cohort consists of 123 patients with newly diagnosed CD and 198 control subjects, further details of which are described in the original paper (Figure 1).<sup>9</sup>

### Samples

Peripheral blood leukocyte DNA was bisulphite converted and DNA methylation profiling was performed using the Illumina HumanMethylation450K platform (Illumina, San Diego, CA). Samples from patients treated with 6-MP or placebo were randomly distributed across chips. A total 41 technical replicates were distributed across chips, runs, and cohorts. Genotype analysis was performed using the Illumina Omni Express Exome (500k SNPs) array for the TOPPIC cohort and the Illumina CoreExome Beadchip array.

### DNA Methylation Analysis

**Data Preprocessing.** DNA methylation data was read from iData using the R package minfi.<sup>55</sup> Estimated cell proportion admixture<sup>56</sup> was obtained using estimateCellCounts function of the same package. The minfi processing stream was then followed: quantile normalization (preprocessQuantile); probes on sex chromosomes were removed (11458 probes), samples with >1% with detection P values >5% (0 samples) were filtered; and methylation probes containing SNPs (dropLociWithSnps, 17,541 probes) and cross-

reactive probes (26,569 probes) were also removed.<sup>57</sup> Batch correction was performed using ComBat for array (72 batches) and subsequently chip position (12 batches). Processing steps were visualized in ShinyMethyl interface.<sup>58</sup> There were no sex mismatches. Forty technical replicates were used across different clips and runs. Technical variation was assessed using MDS plots and intraclass correlation of the top 1000 most variable methylation probes. Technical replicates were removed before downstream analyses.

**DNA Methylation and Risk of Disease Recurrence Following Surgery in Patients With CD.** The composite clinical outcome used in the original TOPPIC trial consisting of an increase in Crohn's disease activity index of more than 150 and an increase of 100 points from baseline measurement together with the institution of immunosuppressive treatment, or further surgery. Secondary outcomes of CD disease recurrence included the highest endoscopic scores (CDEIS, Rutgeerts) measured at 49 and 157 weeks following randomization. TOPPIC data alone were read into R and processed using the previously mentioned steps. DMP analysis (recurrence vs no recurrence) was performed as mentioned with the following covariates: age, sex, smoking status, treatment/placebo, and cell proportions. DVPs were assessed using the iEVORA package using the row\_ievora() function in the matrixTests package with default parameter of a raw t-test threshold of  $P < .05$  and FDR corrected P threshold of Bartlett test step  $<0.001$ .<sup>28</sup> To adjust for covariates, a matrix of the residual values from a linear model of the covariates (age, gender, smoking status, cell



**Table 11.** Functional and Biologic Relevance of Smoking-Related Probes Associated With CD

Probe	Symbol	Function/relevance in IBD
CD-specific smoking-associated methylation probes		
cg24497361	RHOG	Ras homologue family member G. Rho family of small GTPases. Facilitates translocation of a GEF from the cytoplasm to the membrane. Found to be a smoking-related methylation probe by Dugue et al. <sup>30</sup>
cg17777683	CFLAR (cFLIP)	Caspase 8 and FADD-like apoptosis regulator. Regulator of apoptosis. Cigarette smoke decreases bronchial expression and increases susceptibility for cell death and DAMP release. <sup>31</sup> Found to be smoking-related by Sikdar et al. <sup>32</sup>
cg03088955	JOSD1	Josephin containing domain 1. Deubiquitination enzyme. Involved in autophagy. <sup>33</sup>
Table 10 - Top 20 Smoking associated methylation probes.		
cg01218206	SIK2	Salt-induced kinase 2. Enable ATP binding activity. Involved in positive regulation of TORC1 and 2 signaling. Involved in TGF- $\beta$ mediated apoptosis. <sup>34</sup> Found to be a smoking-related methylation probe by Dugue et al. <sup>30</sup>
cg05895711		Found to be a smoking-related methylation probe by Dugue et al. <sup>30</sup>
cg08006672		Seen by Sikdar et al. <sup>32</sup> in a meta-analysis of smoking-related probes to associate with smoking.
cg09273683	PIP4KA2	Phosphatidylinositol-5,4-biphosphate 4 kinase type alpha 2. Kinase involved in secretion, cell proliferation, differentiation, and motility. Linked with schizophrenia and acute myeloid leukemia. A SNP in this region was found to be an environmental interactor between smoking and colorectal cancer. <sup>35</sup>
cg18688062	PSORS1C3	Psoriasis Susceptibility 1 Candidate 3. Found to be a smoking-related methylation probe by Dugue et al. <sup>30</sup>
cg21963318	COX4I1	Cytochrome c oxidase, a mitochondrial enzyme involved in mitochondrial respiration.
Smoking-related probe that intersects with CD vs control DMPs (smoking included as a covariate)		
cg14753356		Found to be smoking related by Sikdar et al. <sup>32</sup> and Dugue et al. <sup>30</sup>
cg00295485	UXS1	Found to be smoking related by Sikdar <sup>32</sup>
cg21963318	COX4I1	Cytochrome c oxidase, as above
Smoking-related probe that intersects with CD vs control DMPs (smoking not a covariate)		
cg13033858	SSH1	Slingshot protein phosphatase 1. Associated with colorectal cancer progression and prognosis. <sup>36</sup> Found to be smoking related by Sikdar et al. <sup>32</sup>

NOTE. Yellow denotes probes not associated with smoking in previous meta-analyses of smoking and methylation (Gao, Sikar, Dugue et al).

CD, Crohn's disease; DAMP, damage associated mucosal patterns; DMP, differentially methylated position; GEF, guanine nucleotide exchange factor; IBD, inflammatory bowel disease; SNP, single-nucleotide polymorphism.

proportions) was used as the input for the DVP iEVORA method. Data were submitted to the DNA methylation Clock Foundation (<https://dnamage.clockfoundation.org/>) for estimation of epigenetic age scores using methods by Horvath,<sup>37</sup> Hannum,<sup>38</sup> phenoAge,<sup>39</sup> tissue specific (skin and blood clock),<sup>40</sup> and GRIMAge.<sup>41</sup> Correlation was made with actual biologic age and estimates of age acceleration were made (methylation age – biologic age). Smoking-associated probes (DMPs) were identified using a linear model of smoking as the outcome (current vs exsmoker/never smoked) with cell proportions as covariates. Smoking-associated probes were correlated with previously published smoking-related probes.<sup>29,59</sup>

### Genotype and meQTL Analysis

Genotypes were called by GenemStudio and data were processed using plink.<sup>60</sup> Data assessed for sex mismatches. meQTLs were identified using the matrixEQTL package.<sup>61</sup> meQTLs were identified using significant DMP and DVP

methylation probes using the modelLinear function with age, sex, and smoking status as covariates to identify meQTLs (MAF >0.1, cis distance of  $1 \times 10^6$ , min  $P$  value  $1 \times 10^6$ )  $P$  values were FDR corrected. For disease-specific meQTLs the modelLinearCross function was used including only significant DMP and DVP methylation probes with the following covariates (age, sex, smoking status) to identify meQTLs associated with disease recurrence in the entire TOPPIC dataset (MAF 0.1, cis distance of  $1 \times 10^6$ , min  $P$  value  $1 \times 10^6$ ).

### Validation of DNA Methylation Changes in IBD Cases and Control Subjects

Raw 450K HumanMethylation iData from IBD BIOM and TOPPIC cohorts were read into R using minfi and both datasets were normalized together using the previously mentioned steps. Batch correction was performed using ComBat for array (72 batches) and chip position (12 batches).<sup>62,63</sup> DMP analysis was performed using limma

comparing CD cases (BIOM and TOPPIC separately) with control subjects (BIOM only<sup>9</sup>).<sup>64</sup> The 2 CD cohorts (BIOM, TOPPIC) were analyzed together against control subjects (BIOM only) (Figure 1). The following covariates were used in linear models (age, sex, smoking status, cell deconvolution values).<sup>65</sup> Correction for multiple testing was performed using the Holm adjusted *P* value.<sup>66</sup> Overlap with previously published DMP lists was assessed for overrepresentation using phyper test for hypergeometric distribution.<sup>67</sup> DMR analysis was performed using DMRcate with an FDR threshold of *P* < .001, Gaussian Kernel Bandwidth lamda of 500, and scaling factor C of 5.<sup>68,69</sup> DVP analysis was performed using the residual matrix of a linear model of covariates (1 ~ age + sex + smoking status + cell counts) with the iEVORA algorithm using the row\_ievora() function in the matrixTests package with default parameter of a raw *t*-test threshold of *P* < .05 and FDR corrected *P* threshold of Bartlett test step <0.001.<sup>39</sup>

## References

- Horvath S, Erhart W, Brosch M, et al. Obesity accelerates epigenetic aging of human liver. *Proc Natl Acad Sci USA* 2014;111:15538–15543.
- Horvath S, Garagnani P, Bacalini MG, et al. Accelerated epigenetic aging in Down syndrome. *Aging cell* 2015;14:491–495.
- Horvath S, Levine AJ. HIV-1 infection accelerates age according to the epigenetic clock. *J Infect Dis* 2015;212:1563–1573.
- Horvath S, Mah V, Lu AT, et al. The cerebellum ages slowly according to the epigenetic clock. *Aging* 2015;7:294–306.
- Ventham NT, Kennedy NA, Nimmo ER, et al. Beyond gene discovery in inflammatory bowel disease: the emerging role of epigenetics. *Gastroenterology* 2013;145:293–308.
- Noble AJ, Nowak JK, Adams AT, et al. Defining interactions between the genome, epigenome, and the environment in inflammatory bowel disease: progress and prospects. *Gastroenterology* 2023;165:44–60.e2.
- Nimmo ER, Prendergast JG, Aldhous MC, et al. Genome-wide methylation profiling in Crohn's disease identifies altered epigenetic regulation of key host defense mechanisms including the Th17 pathway. *Inflamm Bowel Dis* 2012;18:889–899.
- Adams AT, Kennedy NA, Hansen R, et al. Two-stage genome-wide methylation profiling in childhood-onset Crohn's disease implicates epigenetic alterations at the VMP1/MIR21 and HLA loci. *Inflamm Bowel Dis* 2014;20:1784–1793.
- Ventham NT, Kennedy NA, Adams AT, et al. Integrative epigenome-wide analysis demonstrates that DNA methylation may mediate genetic risk in inflammatory bowel disease. *Nat Commun* 2016;7:13507.
- Kalla R, Adams AT, Nowak JK, et al. Analysis of systemic epigenetic alterations in inflammatory bowel disease: defining geographical, genetic and immune-inflammatory influences on the circulating methylome. *J Crohns Colitis* 2023;17:170–184.
- Biasci D, Lee JC, Noor NM, et al. A blood-based prognostic biomarker in IBD. *Gut* 2019;68:1386–1395.
- Lee JC, Biasci D, Roberts R, et al. Genome-wide association study identifies distinct genetic contributions to prognosis and susceptibility in Crohn's disease. *Nat Genet* 2017;49:262–268.
- Somineni HK, Venkateswaran S, Kilaru V, et al. Blood-derived DNA methylation signatures of Crohn's disease and severity of intestinal inflammation. *Gastroenterology* 2019;156:2254–2265.
- Marigorta UM, Denson LA, Hyams JS, et al. Transcriptional risk scores link GWAS to eqtls and predict complications in Crohn's disease. *Nat Genet* 2017;49:1517–1521.
- Kugathasan S, Denson LA, Walters TD, et al. Prediction of complicated disease course for children newly diagnosed with Crohn's disease: a multicentre inception cohort study. *Lancet* 2017;389:1710–1718.
- Frolkis AD, Dykeman J, Negrón ME, et al. Risk of surgery for inflammatory bowel diseases has decreased over time: a systematic review and meta-analysis of population-based studies. *Gastroenterology* 2013;145:996–1006.
- Jenkinson PW, Plevris N, Siakavellas S, et al. Temporal trends in surgical resection rates and biologic prescribing in Crohn's disease: a population-based cohort study. *J Crohns Colitis* 2020;14:1241–1247.
- Mowat C, Arnott I, Cahill A, et al. Mercaptopurine versus placebo to prevent recurrence of Crohn's disease after surgical resection (TOPPIC): a multicentre, double-blind, randomised controlled trial. *Lancet Gastroenterol Hepatol* 2016;1:273–282.
- Shen J, Zhao J, Ye QY, et al. Interference of mir-943-3p with secreted frizzled-related proteins4 (sfrp4) in an asthma mouse model. *Cell Tissue Res* 2019;378:67–80.
- Yaman E, Gasper R, Koerner C, et al. Rasgef1a and rasgef1b are guanine nucleotide exchange factors that discriminate between RAP GTP-binding proteins and mediate rap2-specific nucleotide exchange. *FEBS J* 2009;276:4607–4616.
- Perez White BE, Getsios S. EPH receptor and ephrin function in breast, gut, and skin epithelia. *Cell Adh Migr* 2014;8:327–338.
- Hafner C, Meyer S, Langmann T, et al. Ephrin-b2 is differentially expressed in the intestinal epithelium in Crohn's disease and contributes to accelerated epithelial wound healing in vitro. *World J Gastroenterol* 2005;11:4024–4031.
- Fenton CG, Taman H, Florholmen J, et al. Transcriptional signatures that define ulcerative colitis in remission. *Inflamm Bowel Dis* 2021;27:94–105.
- Grandi A, Zini I, Palese S, et al. Targeting the EPH/ephrin system as anti-inflammatory strategy in IBD. *Front Pharmacol* 2019;10:691.
- Howell KJ, Kraiczky J, Nayak KM, et al. DNA methylation and transcription patterns in intestinal epithelial cells from pediatric patients with inflammatory bowel diseases differentiate disease subtypes and associate with outcome. *Gastroenterology* 2018;154:585–598.
- Cappello F, David S, Rappa F, et al. The expression of hsp60 and hsp10 in large bowel carcinomas with lymph node metastase. *BMC Cancer* 2005;5:139.

27. Melle C, Bogumil R, Ernst G, et al. Detection and identification of heat shock protein 10 as a biomarker in colorectal cancer by protein profiling. *Proteomics* 2006; 6:2600–2608.
28. Teschendorff AE, Gao Y, Jones A, et al. DNA methylation outliers in normal breast tissue identify field defects that are enriched in cancer. *Nat Commun* 2016;7:10478.
29. Gao X, Jia M, Zhang Y, et al. DNA methylation changes of whole blood cells in response to active smoking exposure in adults: a systematic review of DNA methylation studies. *Clin Epigenetics* 2015;7:113.
30. Dugué PA, Jung CH, Joo JE, et al. Smoking and blood DNA methylation: an epigenome-wide association study and assessment of reversibility. *Epigenetics* 2020; 15:358–368.
31. Faiz A, Heijink IH, Vermeulen CJ, et al. Cigarette smoke exposure decreases CFLAR expression in the bronchial epithelium, augmenting susceptibility for lung epithelial cell death and damp release. *Sci Rep* 2018;8:12426.
32. Sikdar S, Joehanes R, Joubert BR, et al. Comparison of smoking-related DNA methylation between newborns from prenatal exposure and adults from personal smoking. *Epigenomics* 2019;11:1487–1500.
33. Tian S, Jin S, Wu Y, et al. High-throughput screening of functional deubiquitinating enzymes in autophagy. *Autophagy* 2021;17:1367–1378.
34. Hutchinson LD, Darling NJ, Nicolaou S, et al. Salt-inducible kinases (siks) regulate  $\text{tgf}\beta$ -mediated transcriptional and apoptotic responses. *Cell Death Dis* 2020;11:49.
35. Sun J, Wang L, Zhou X, et al. Cross-cancer pleiotropic analysis identifies three novel genetic risk variants for colorectal cancer. *Hum Mol Genet* 2023;32:2093–2102.
36. Song X, Xie D, Xia X, et al. Role of *ssh1* in colorectal cancer prognosis and tumor progression. *J Gastroenterol Hepatol* 2020;35:1180–1188.
37. Horvath S. DNA methylation age of human tissues and cell types. *Genome Biol* 2013;14:R115.
38. Hannum G, Guinney J, Zhao L, et al. Genome-wide methylation profiles reveal quantitative views of human aging rates. *Mol Cell* 2013;49:359–367.
39. Levine ME, Lu AT, Quach A, et al. An epigenetic biomarker of aging for lifespan and healthspan. *Aging* 2018;10:573–591.
40. Horvath S, Oshima J, Martin GM, et al. Epigenetic clock for skin and blood cells applied to Hutchinson Gilford progeria syndrome and ex vivo studies. *Aging* 2018; 10:1758–1775.
41. Lu AT, Quach A, Wilson JG, et al. DNA methylation grimage strongly predicts lifespan and healthspan. *Aging* 2019;11:303–327.
42. Joustra VW, Li Yim AYW, de Bruyn JR, et al. Peripheral blood DNA methylation profiles do not predict endoscopic post-operative recurrence in Crohn's disease patients. *Int J Mol Sci* 2022;23:10467.
43. Webster AP, Plant D, Ecker S, et al. Increased DNA methylation variability in rheumatoid arthritis-discordant monozygotic twins. *Genome Med* 2018;10:64.
44. Paul DS, Teschendorff AE, Dang MA, et al. Increased DNA methylation variability in type 1 diabetes across three immune effector cell types. *Nat Commun* 2016;7: 13555.
45. To N, Gracie DJ, Ford AC. Systematic review with meta-analysis: the adverse effects of tobacco smoking on the natural history of Crohn's disease. *Aliment Pharmacol Ther* 2016;43:549–561.
46. Lunney PC, Kariyawasam VC, Wang RR, et al. Smoking prevalence and its influence on disease course and surgery in Crohn's disease and ulcerative colitis. *Aliment Pharmacol Ther* 2015;42:61–70.
47. Reese GE, Nanidis T, Borysiewicz C, et al. The effect of smoking after surgery for Crohn's disease: a meta-analysis of observational studies. *Int J Colorectal Dis* 2008;23:1213–1221.
48. Wang C, Ni W, Yao Y, et al. DNA methylation-based biomarkers of age acceleration and all-cause death, myocardial infarction, stroke, and cancer in two cohorts: the NAS, and KORA F4. *EBioMedicine* 2021;63:103151.
49. Marioni RE, Shah S, McRae AF, et al. DNA methylation age of blood predicts all-cause mortality in later life. *Genome Biol* 2015;16:25.
50. McCrory C, Fiorito G, Hernandez B, et al. Grimace outperforms other epigenetic clocks in the prediction of age-related clinical phenotypes and all-cause mortality. *J Gerontol A Biol Sci Med Sci* 2020;76:741–749.
51. Sadahiro R, Knight B, James F, et al. Major surgery induces acute changes in measured DNA methylation associated with immune response pathways. *Sci Rep* 2020;10:5743.
52. Poganik JR, Zhang B, Baht GS, et al. Biological age is increased by stress and restored upon recovery. *Cell Metab* 2023;35:807–820.
53. Heyn H, Moran S, Hernando-Herraez I, et al. DNA methylation contributes to natural human variation. *Genome Res* 2013;23:1363–1372.
54. Palumbo D, Affinito O, Monticelli A, et al. DNA methylation variability among individuals is related to CPGS cluster density and evolutionary signatures. *BMC Genomics* 2018;19:229.
55. Aryee MJ, Jaffe AE, Corrada-Bravo H, et al. Minfi: a flexible and comprehensive bioconductor package for the analysis of infinium DNA methylation microarrays. *Bioinformatics* 2014;30:1363–1369.
56. Houseman EA, Accomando WP, Koestler DC, et al. DNA methylation arrays as surrogate measures of cell mixture distribution. *BMC Bioinformatics* 2012;13:86.
57. Chen Y-a, Lemire M, Choufani S, et al. Discovery of cross-reactive probes and polymorphic CPGS in the illumina infinium humanmethylation450 microarray. *Epigenetics* 2013;8:203–209.
58. Fortin JP, Fertig E, Hansen K. Shinymethyl: interactive quality control of illumina 450k DNA methylation arrays in R. *F1000Res* 2014;3:175.
59. Tsaprouni LG, Yang TP, Bell J, et al. Cigarette smoking reduces DNA methylation levels at multiple genomic loci but the effect is partially reversible upon cessation. *Epigenetics* 2014;9:1382–1396.
60. Purcell S, Neale B, Todd-Brown K, et al. Plink: a tool set for whole-genome association and population-based linkage analyses. *Am J Hum Genet* 2007;81:559–575.

61. Shabalina AA. Matrix eqtl: ultra fast EQTL analysis via large matrix operations. *Bioinformatics* 2012;28:1353–1358.
62. Johnson WE, Li C, Rabinovic A. Adjusting batch effects in microarray expression data using empirical bayes methods. *Biostatistics* 2007;8:118–127.
63. Leek JT, Johnson WE, Parker HS, et al. The SVA package for removing batch effects and other unwanted variation in high-throughput experiments. *Bioinformatics* 2012;28:882–823.
64. Smyth GK. Limma: linear models for microarray data. In: Gentleman R, Carey V, Dudoit S, et al., eds. *Bioinformatics and computational biology solutions using {R} and bioconductor*. New York: Springer, 2005: 397–420.
65. Ritchie ME, Phipson B, Wu D, et al. Limma powers differential expression analyses for RNA-sequencing and microarray studies. *Nucleic Acids Res* 2015;43:e47.
66. Holm S. A simple sequentially rejective multiple test procedure. *Scand J Stat* 1979;6:65–70.
67. Rivals I, Personnaz L, Taing L, et al. Enrichment or depletion of a go category within a class of genes: which test? *Bioinformatics* 2007;23:401–407.
68. Mallik S, Odom GJ, Gao Z, et al. An evaluation of supervised methods for identifying differentially methylated regions in Illumina methylation arrays. *Brief Bioinform* 2019;20:2224–2235.
69. Peters TJ, Buckley MJ, Statham AL, et al. De novo identification of differentially methylated regions in the human genome. *Epigenetics Chromatin* 2015;8:6.

Bloom, Mohamed Yousif, Linzi Thomas, Simon Campbell, Stephen J. Lewis, Shaji Sebastian, Sandip Sen, Simon Lal, Chris Hawkey, Charles Murray, Fraser Cummings, Jason Goh, James O. Lindsay, Naila Arebi, Lindsay Potts, Aileen J. McKinley, John M. Thomson, John A. Todd, Mhairi Colлие, Ashley Mowat, Daniel R. Gaya, Jack Winter, Graham D. Naismith, Catriona Keerie, Steff Lewis, and Robin J. Prescott.

The IBD-BIOM Consortium includes Gordan Lauc, Harry Campbell, Dermot P.B. McGovern, Vito Annese, Vlatka Zoldoš, Iain K. Permberton, Manfred Wuhler, Daniel Kolarich, Daryl L. Fernandes, Evropi Theodorou, Victoria Merrick Daniel I. Spencer, Richard A. Gardner, Ray Doran, Archana Shubhakar, Ray Boyapati, Igor Rudan, Paolo Lionetti, Irena Trbojević Akmačić, Jasminka Krišić, Frano Vučković, Jerko Štambuk, Mislav Novokmet, Maja Pučić-Baković, Olga Gornik, Angelo Andriulli, Laura Cantoro, Giancarlo Sturniolo, Gionata Fiorino, Natalia Manetti, Anna Latiano, Anna Kohn, Renata D'Inca, Silvio Danese, Colin L. Noble, Charlie W. Lees, Alan G. Shand, Gwo-Tzer Ho, Lee Murphy, Jude Gibson, Louise Evenden, Nicola Wrobel, Tamara Gilchrist, Angie Fawkes, Guinevere S.M. Kammeijer, Florent Clerc, Noortje de Haan, Aleksandar Vojta, Ivana Samaržija, Dora Markulin, Marija Klasić, Paula Dobrinčić, Yurii Aulchenko, Tim van den Heuve, Daisy Jonkers, and Marieke Pierik.

#### CRediT Authorship Contributions

Nicholas T. Ventham (Formal analysis: Lead; Writing – original draft: Lead; Writing – review & editing: Lead)

Nicholas A. Kennedy, PhD (Conceptualization: Equal; Data curation: Equal; Formal analysis: Equal; Project administration: Equal)

Rahul Kalla, PhD (Conceptualization: Supporting; Writing – original draft: Equal; Writing – review & editing: Equal)

Alex T. Adams (Methodology: Supporting; Writing – original draft: Supporting; Writing – review & editing: Equal)

Alexandra J. Noble (Formal analysis: Supporting; Methodology: Supporting; Writing – original draft: Supporting; Writing – review & editing: Supporting)

Holly Ennis (Data curation: Lead; Project administration: Lead; Writing – review & editing: Equal)

TOPPIC Study group (Data curation: Equal; Funding acquisition: Equal; Resources: Equal)

IBD-BIOM Consortium (Conceptualization: Equal; Data curation: Equal; Funding acquisition: Equal)

Craig Mowat (Conceptualization: Equal; Data curation: Equal; Writing – review & editing: Equal)

Malcolm G. Dunlop (Supervision: Equal; Writing – review & editing: Equal)

Jack Satsangi (Conceptualization: Lead; Data curation: Lead; Funding acquisition: Lead; Writing – review & editing: Equal)

#### Conflicts of interest

The authors disclose no conflicts.

#### Funding

This research was funded in whole, or in part, by the Wellcome Trust [Grant number WT097943MA]. For the purpose of open access, the author has applied a CC BY public copyright licence to any Author Accepted Manuscript version arising from this submission TOPPIC Trial was supported by the Medical Research Council, National Institute of Health Research's Efficacy and Mechanism Evaluation Programme, Scottish Government Chief Scientist Office, and the National Institute of Health Research National Portfolio. IBD-BIOM was supported by EU FP7 grants: European Commission IBD-BIOM (contract # 305479), IBD-CHARACTER (contract # 2858546).

Received August 4, 2022. Accepted June 2, 2023.

#### Correspondence

Address correspondence to: Nicholas T. Ventham, PhD, MRCS(Eng), MBBS, Academic Coloproctology, Centre for Genomic and Experimental Medicine, The University of Edinburgh, Edinburgh, Midlothian EH4 6XU, United Kingdom. e-mail: [nventham@ed.ac.uk](mailto:nventham@ed.ac.uk).

#### Acknowledgments

The TOPPIC Study Group includes Ian Arnott, Aiden Cahill, Malcolm Smith, Tariq Ahmad, Sreedhar Subramanian, Simon Travis, John Morris, John Hamlin, Anjan Dhar, Chuka Nwokolo, Cathryn Edwards, Tom Creed, Stuart